



Modelling of gas clathrate hydrate equilibria using the electrolyte non-random two-liquid (eNRTL) model

Matthias Kwaterski, Jean-Michel Herri

► To cite this version:

Matthias Kwaterski, Jean-Michel Herri. Modelling of gas clathrate hydrate equilibria using the electrolyte non-random two-liquid (eNRTL) model. *Fluid Phase Equilibria*, 2014, 371, pp.22-40. 10.1016/j.fluid.2014.02.032 . hal-00978703

HAL Id: hal-00978703

<https://hal.science/hal-00978703>

Submitted on 14 Apr 2014

HAL is a multi-disciplinary open access archive for the deposit and dissemination of scientific research documents, whether they are published or not. The documents may come from teaching and research institutions in France or abroad, or from public or private research centers.

L'archive ouverte pluridisciplinaire **HAL**, est destinée au dépôt et à la diffusion de documents scientifiques de niveau recherche, publiés ou non, émanant des établissements d'enseignement et de recherche français ou étrangers, des laboratoires publics ou privés.

Modelling of Gas Clathrate Hydrate Equilibria using the Electrolyte Non-Random Two-Liquid (eNRTL) Model

Matthias Kwaterski^{1,*} and Jean-Michel Herri^{1,†}

¹Centre SPIN, Département Propice, UMR CNRS 5307 LGF, École Nationale Supérieure des Mines de Saint-Etienne, France

Abstract

Calculations on solid (S)-liquid (L_w)-gas (G)-phase equilibria of selected ternary {water + salt + gas} and quaternary {water + salt₁ + salt₂ + gas} systems (salt = NaCl, KCl, CaCl₂; gas = CH₄, CO₂) comprising a gas clathrate hydrate phase ($S \equiv H$) have been performed. The thermodynamic description of the liquid phase non-idealities observed in these systems has been provided by means of the semi-empirical electrolyte NRTL (eNRTL) excess Gibbs energy model. Multicomponent expressions for individual as well as mean ionic activity coefficients as defined by both, a previous and the most recent version of the eNRTL model, have been implemented in a computer programme written in the Java programming language. Basic model parameters are provided by means of a data bank set up in the xml file format. The correctness of the programme implementation of the eNRTL expressions has been verified by comparing the results of selected example calculations with corresponding results given in the original literature sources. The programme code of the model implementation has been incorporated into a previously developed in-house programme enabling to perform equilibrium calculations on non-electrolyte aqueous systems involving gas hydrate phases. In the H- L_w -G calculations, fugacities in the gas phase were calculated by means of the Soave-Redlich-Kwong (SRK) equation of state (EOS), whereas a Henry's law approach in combination with the eNRTL model has been applied to characterise the liquid phase. The van der Waals and Platteeuw model has been used to describe the gas clathrate hydrate phase. A satisfying predictive description of the experimental p - T -H- L_w -G phase equilibrium data is achieved with average absolute relative deviations (AARD) between experimental and calculated pressures ranging from 1 % to 15 %.

Keywords: Modelling, gas hydrate, eNRTL model, electrolytes, phase equilibrium, CO₂, CH₄

* Corresponding author: Phone: +33 (0) 4 77 42 00 62, Fax: +33 (0) 4 77 49 96 92, e-mail: kwaterski@emse.fr

† Phone: +33 (0) 4 77 42 02 92, Fax +33 (0) 4 77 49 96 92, e-mail: herri@emse.fr

1 Introduction **Formelabschnitt 1**

Gas clathrate hydrates are mixed solid crystalline phases which are built up by a network of hydrogen bonded water molecules comprising cage-like structural units, each of which can encapsulate a single appropriately sized guest molecule. The guest species, generally molecules of low molecular weight gases and organic compounds [1], stabilise the solid solvent, the thermodynamically metastable host lattice, by interacting with the water molecules of the cavities through van der Waals forces [2]. Gas clathrate hydrates are thermodynamically stable in regions of ambient or lower temperatures (near the normal freezing point of water) and elevated pressures (typically more than 0.6 MPa) [3,4] and crystallise in the two cubic structures I (sI) and II (sII), and the hexagonal structure H (sH). Besides having the potential for numerous applications in the oil and gas industry and the energy sector (e.g. in gas storage and separation, air-conditioning systems and water desalination and treatment [5]), gas hydrates can also cause problems in the oil and gas industry (e.g. pipeline blockages by hydrates in drilling applications or gas pipelines) [6]. Species being capable of forming hydrogen bonds with the water molecules like methanol or ethylene glycol as well as water-soluble polymers or electrolytes are known for acting as thermodynamic inhibitors with respect to the formation of gas hydrates [3]. These additives can prevent the formation of hydrate plugs by altering the state of the liquid phase [3] and thereby changing the phase transition conditions [7].

Due to the electrostatic forces acting between ions the thermodynamic description of electrolyte solutions is significantly more difficult than the treatment of non-electrolyte systems [8,9]. To model electrolyte solutions, an electrolyte equation of state (EOS), especially useful at high pressures, an excess Gibbs energy model [8] or a combination of the two strategies is usually employed. Several electrolyte EOS, like e.g. the Fürst-Renon EOS [10,11], the electrolyte modification [8] of the Trebble-Bishnoi EOS [12,13], or the statistical associating fluid theory with variable range for electrolytes (SAFT-VRE) EOS [14] have been developed. Besides, numerous semi-empirical excess Gibbs energy models have been proposed [15], as e.g. the model of Bromley [16], the ion-interaction model of Pitzer [17,18], the model of Cruz and Renon [19], the eNRTL-model of Chen et al. [15,20-23], the LIQUAC- model of Li et al. [24] and the MSA-model of Papaiconomou et al. [25].

To model the Hydrate (H)-Liquid (L_w)-Gas (G)-phase boundary in systems containing electrolytes, an equation of state and/or activity coefficient approach for the fluid phases is combined with the hydrate model of van der Waals and Platteeuw (vdW-P) [26]. Englezos and Bishnoi [27] e.g. presented an approach to predict the thermodynamic gas hydrate formation conditions in aqueous systems containing light hydrocarbon gases and single or mixed electrolytes using Pitzer's [17] and Meissner's [28] activity coefficient models. Clarke and Bishnoi [8] have developed an electrolyte EOS for mixed salt and mixed solvent systems to describe the Liquid-Vapour- (L-V-) equilibrium in these mixtures. The EOS was also used to model the H-L-V-equilibrium obtained in systems containing additionally one or more of the gases CH_4 , CO_2 , H_2S and/or C_3H_8 [8]. Hsieh et al. [7] presented an approach for modelling the change in hydrate forming conditions in mixtures containing electrolytes and molecular inhibitors. They combined the vdW-P model with the Peng-Robinson-Stryjek-Vera EOS [29], using the first order modified Huron-Vidal (MHV1) mixing rule [30] with two activity coefficient models, the UNIQUAC [31] and the COSMO-SAC [32,33] model.

Prior to initiating the current modelling work, incipient gas hydrate forming conditions in non-electrolyte aqueous systems were modelled in our research group. The calculations were

performed with our in-house programme named “GasHyDyn” which was created and described earlier [34] using the object oriented programming language Java. The programme has been based on the algorithm proposed by Sloan [35] and its code is available from the second author on request. The need for extending this in-house programme to enable the treatment of electrolyte systems originated from the attempt to model the thermodynamics of so-called (gas-)semiclathrate hydrates of tri-*n*-butylammonium bromide (TBAB), the results of which will be dealt with in a forthcoming article [36]. Since TBAB dissociates into ions in aqueous solution, an electrolyte model was required to describe the liquid phase non-idealities in this system with sufficient accuracy. Bèlvèze et al. [37] showed that the eNRTL-model [20,21] does an excellent job in describing experimental data on the mean molal activity coefficient of TBAB, $\gamma_{b, \text{TBAB}, \pm}^*$, in aqueous solution at 298.15 K [38] over a wide range of TBAB concentration (maximum overall molality $\bar{b}_{\text{TBAB}, \text{max}} = 27 \text{ mol kg}^{-1}$, residual standard deviation of $\sigma = 0.038$ with respect to calculated and measured results on $\ln \gamma_{b, \text{TBAB}, \pm}^*$). Moreover, only two parameters are required for the isothermal description of single electrolyte solutions with this model [20,21] (e.g. the famous Pitzer model [17] needs three). Therefore we decided to use the eNRTL-model to describe the isobaric H-L_w equilibrium in the system {H₂O + TBAB} and H-L_w-G-equilibria in the corresponding gas semi-clathrate hydrate systems. In this preliminary study the aim is to test the suitability of the model to describe systems with conventional gas hydrate phases in the presence of electrolytes. Therefore, a Java implementation of both the previous [21] and the updated version of the single-solvent multicomponent eNRTL-model [23] was created initially. After having thoroughly tested the correctness of the eNRTL-code, the programme was incorporated into our previously existing in-house programme for modelling H-L_w-G-phase equilibria. Subsequently, by means of the new programme, incipient gas hydrate formation conditions were modelled in systems with sodium chloride (NaCl) and potassium chloride (KCl) or calcium chloride (CaCl₂) and the gases methane (CH₄) or carbon dioxide (CO₂).

2 Modelling approach **Formelabschnitt (nächster)**

2.1 Hydrate-liquid-gas equilibrium

Thermodynamic equilibrium between the gas hydrate phase (H) and the aqueous liquid phase (L_w) under incipient hydrate formation conditions, when being in simultaneous equilibrium with a gas phase (G), can be expressed by

$$\Delta_{\beta}^{\text{H}} \mu_{\text{w}} = \Delta_{\beta}^{\text{L}_w} \mu_{\text{w}} \quad (1)$$

where $\Delta_{\beta}^{\text{H}} \mu_{\text{w}} \equiv \mu_{\text{w}}^{\text{H}} - \mu_{\text{w}}^{\circ, \beta}$ denotes the difference in the chemical potential of water in the gas hydrate phase and the pure (index \circ) solid solvent phase, i.e. the empty metastable hydrate lattice (index β). Similarly, $\Delta_{\beta}^{\text{L}_w} \mu_{\text{w}} \equiv \mu_{\text{w}}^{\text{L}_w} - \mu_{\text{w}}^{\circ, \beta}$ designates the chemical potential difference of water in the liquid and the empty hydrate phase. It should be pointed out that the way for expressing the equilibrium condition in eq. (1) differs from the way it is usually found in the literature, firstly because minuend and subtrahend are reversed as it was also done by Ballard and Sloan [39] (i.e., $\mu_{\text{w}}^{\pi} - \mu_{\text{w}}^{\circ, \beta}$ instead of $\mu_{\text{w}}^{\circ, \beta} - \mu_{\text{w}}^{\pi}$ with $\pi = \text{H}, \text{L}_w$), and secondly, because the nomenclature is adopted from the notation as recommended by the IUPAC Commission I.2. [40]. Since the presence of water in the gas phase was neglected in a good approximation, the condition involving the chemical potential of water in this phase was not considered.

2.2 The thermodynamic description of the hydrate phase

The clathrate hydrate phase is described by means of the ideal solid solution theory of van der Waals and Platteeuw [26]. In this statistical thermodynamic model, the chemical potential difference $\Delta_{\beta}^H \mu_w$, expressed on a molar basis, is given by

$$\frac{\Delta_{\beta}^H \mu_w}{RT} = \sum_{i \in S_{\text{cav}}} \nu_i \ln \left(1 - \sum_{j \in S_g} \theta_{ji}^H \right) \quad (2)$$

In eq. (2), R denotes the universal gas constant [41], $S_{\text{cav}} = \{1, \dots, N_{\text{cav}}\}$ the set of indices of the N_{cav} different types of cavities, and $S_g = \{1, \dots, N_g\}$ the set of indices identifying the N_g different types of guest species. ν_i is the number of type i cavities per water molecule, and θ_{ji}^H the fractional occupancy of guest j in cavity i in the hydrate phase. θ_{ji}^H can be expressed in terms of the Langmuir constant C_{ji} of guest j in cavity i , and the fugacity f_j of j as

$$\theta_{ji}^H = \frac{C_{ji} f_j}{1 + \sum_{j' \in S_g} C_{ji} f_{j'}} \quad (\text{for all } j \in S_g \text{ and } i \in S_{\text{cav}}) \quad (3)$$

The expression in eq. (3) resembles the well known relation describing the two dimensional adsorption according to the Langmuir model. At H-L_w-G-equilibrium, the isofugacity criterion, implicitly incorporated into eq. (2) [27] does hold. The latter states the equality of the fugacities f_j throughout the co-existing phases, i.e. $f_j^H = f_j^{L_w} = f_j^G (\equiv f_j)$. Hence, any of the f_j 's in one of the three phases may be employed for calculating f_j . For practical reasons, the gas phase fugacities f_j^G , obtained from the SRK-EOS [42], were used for this purpose.

The Langmuir constants were calculated from an expression proposed by Parrish and Prausnitz [43] describing the cell potential energy of guest j within the spherically assumed cavity i of water molecules. The latter in turn is based on the Kihara core potential [44] which accounts for the single interactions between the guest and each of the water molecules constituting the cavity [1]. In that way, C_{ji} is given in terms of the Kihara parameters σ_{jw} , ϵ_{jw} and a_j , the core distance at which attraction and repulsion of a guest host-pair balance each other, the corresponding characteristic energy, and the core radius of the guest molecule, respectively, and the lattice specific quantities z_i and R_i , the coordination number and the radius of the cavity i , respectively [1]. The relations $C_{ji} = f(a_j, \sigma_{jw}, \epsilon_{jw}, z_i, R_i)$ in which the water molecules are assigned a zero core radius (i.e., $a_w = 0 \Rightarrow 2a_{jw} = a_j$) [45] are compiled in appendix A.1. The values for a_j , σ_{jw} and ϵ_{jw} used in this study are listed in Table 6 along with literature data on σ_{jw} and ϵ_{jw} . The values for z_i and R_i were taken from [35].

2.3 Dependence of the liquid phase chemical potential difference on the state variables

The model description for $\Delta_{\beta}^{L_w} \mu_w$ as function of temperature T , pressure p and the vector of independent mole fractions \vec{x}^{L_w} , was provided by the following equation

$$\begin{aligned} \frac{\Delta_{\beta}^{L_w} \mu_w(T, p, \vec{x}^{L_w})}{RT} &= \frac{\Delta_{\beta}^{L_w} \mu_w^{\circ}(T_0, p_0)}{RT_0} + \frac{bT_0 + \Delta_{\beta}^{L_w} C_{p,m,w}^{\circ}(T_0, p_0)}{R} \ln \left(\frac{T_0}{T} \right) + \frac{b}{2R} (T - T_0) \\ &+ \frac{1}{R} \left(\frac{\Delta_{\beta}^{L_w} H_{m,w}^{\circ}(T_0, p_0)}{T_0} - \Delta_{\beta}^{L_w} C_{p,m,w}^{\circ}(T_0, p_0) - \frac{b}{2} T_0 \right) \left(\frac{T_0}{T} - 1 \right) \\ &+ \frac{\Delta_{\beta}^{L_w} V_{m,w}^{\circ}(T_0, p_0)}{RT} (p - p_0) - \ln \gamma_{x,w}^{L_w}(T, p, \vec{x}^{L_w}) - \ln x_w^{L_w} \end{aligned} \quad (4)$$

where $x_w^{L_w}$ and $\gamma_{x,w}^{L_w}$ denotes the mole fraction and the activity coefficient of water in the liquid phase, respectively. $\Delta_\beta^{L_w} \mu_w^\circ(T_0, p_0)$, $\Delta_\beta^{L_w} H_{m,w}^\circ(T_0, p_0)$, $\Delta_\beta^{L_w} C_{p,m,w}^\circ(T_0, p_0)$ and $\Delta_\beta^{L_w} V_{m,w}^\circ(T_0, p_0)$ are the difference in chemical potential, molar enthalpy, isobaric molar heat capacity and molar volume between water in the pure liquid and the pure metastable hydrate phase under reference conditions for temperature and pressure of $T_0 = 273.15$ K and $p_0 = 0$ MPa [34], respectively. Along with the empirical constant b , these quantities are regarded as parameters determined by using various experimental and calculation techniques [35]. Eq. (4) is derived from an empirical expression for $\Delta_\beta^{L_w} C_{p,m,w}^\circ$, which was e.g. also used by Holder et al. [46], via classical thermodynamic relationships (Appendix A.2).

The reference parameters describing the phase change $\beta \rightarrow L_w$ were taken from different literature sources [35,47-49] as compiled in Table 1. Since the data available for $\Delta_\beta^{L_w} \mu_w^\circ(T_0, p_0)$ show strong variations among different laboratories [34], this parameter needs to be selected with precaution when being used in calculations of C_{ji} along with a given set of Kihara parameters [34]. A great variation is also detected among the values published for $\Delta_\beta^{L_w} H_{m,w}^\circ(T_0, p_0)$. In contrast, literature data on $\Delta_\beta^{L_w} C_{p,m,w}^\circ(T_0, p_0)$, b and $\Delta_\beta^{L_w} V_{m,w}^\circ(T_0, p_0)$ are less numerous. Based on the conclusions drawn in [34], the data of Handa and Tse [49] were used for $\Delta_\beta^{L_w} \mu_w^\circ(T_0, p_0)$ and $\Delta_\beta^{L_w} H_{m,w}^\circ(T_0, p_0)$. The value for $\Delta_\beta^{L_w} V_{m,w}^\circ(T_0, p_0)$ was taken from John et al. [48], while the values for $\Delta_\beta^{L_w} C_{p,m,w}^\circ(T_0, p_0)$ and b were taken from Sloan [35].

Table 1 Parameters characterising the phase change between the “empty” hydrate phase β and the pure liquid water phase L_w

	sI	sII
$\Delta_\beta^{L_w} \mu_w^\circ(T_0, p_0) / \text{J mol}^{-1}$ ^a	-1263 ^c -1297 ^d -1120 ^e 1287 ^f	-883.8 ^c -937 ^d -931 ^e -1068 ^f
$\Delta_\beta^{L_w} H_{m,w}^\circ(T_0, p_0) / \text{J mol}^{-1}$ ^{a, b}	4622 ^c 4622 ^d 4297 ^e 5080 ^f	4986 ^c 4986 ^d 4611 ^e 5247 ^f
$\Delta_\beta^{L_w} C_{p,m,w}^\circ(T_0, p_0) / \text{J K}^{-1} \text{mol}^{-1}$ ^a	38.12 ^c	38.12 ^c
$b / \text{J K}^{-2} \text{mol}^{-1}$ ^a	-0.141 ^c	-0.141 ^c
$\Delta_\beta^{L_w} V_{m,w}^\circ(T_0, p_0) / \text{cm}^3 \text{mol}^{-1}$ ^a	-4.5959 ^e	-4.99644 ^e

^a The numerical values for the parameters compiled here are the negative values of the values given in the original sources due to the inversely defined differences as outlined in the text.

^b Since the original data are given as $\Delta_I^\beta H_{m,w}^\circ(T_0, p_0)$, the $\Delta_\beta^{L_w} H_{m,w}^\circ(T_0, p_0)$ -values presented here are derived by adding the molar enthalpy of fusion $\Delta_{\text{fus}} H_{m,w}^\circ(T_0, p_0) = \Delta_I^\beta H_{m,w}^\circ(T_0, p_0) = 6011 \text{ J mol}^{-1}$ [48] to $-\Delta_I^\beta H_{m,w}^\circ(T_0, p_0)$.

^c 2nd ed. of the monograph of Sloan [35].

^d Dharmawardhana [47].

^e John et al. [48]. Since the authors present $\Delta_I^\beta V_{m,w}^\circ(T_0, p_0)$, the value the molar volume of fusion of ice, $\Delta_{\text{fus}} V_{m,w}^\circ(T_0, p_0) = \Delta_I^\beta V_{m,w}^\circ(T_0, p_0) = -1.6 \text{ cm}^3 \text{mol}^{-1}$, as determined from X-ray diffraction data of von Stackelberg and Müller [50], has been added to $-\Delta_I^\beta V_{m,w}^\circ(T_0, p_0)$ for obtaining $\Delta_\beta^{L_w} V_{m,w}^\circ(T_0, p_0)$.

^f Handa and Tse [49].

2.4 The solubility of the gases in the aqueous liquid phase

The solubility of gas j ($j = \text{CH}_4, \text{CO}_2$) in the liquid phase, expressed in terms of the mole fraction $x_j^{\text{L}_w}$, is estimated via a Henry's law approach. Hereby, the assumption was made that the activity coefficient of j , $\gamma_{x,j}^{*,\text{L}_w}$, i.e. the so-called salting-in or salting-out effect [9], can be neglected. Setting $\gamma_{x,j}^{*,\text{L}_w} = 1$ and assuming that the partial molar volume $V_{m,j}^{\infty,\text{L}_w}$ of j at infinite dilution is independent of pressure, the phase equilibrium condition reads [35]

$$f_j^{\text{G}} = f_j^{\text{L}_w} = x_j^{\text{L}_w} k_{\text{H},j,w}(T, p_w^{\sigma}) \exp\left(\frac{p V_{m,j}^{\infty,\text{L}_w}}{RT}\right) \quad (5)$$

where f_j^{G} is the fugacity of j in the gas phase which is calculated by means of the Soave-Redlich-Kwong EOS [42] and $k_{\text{H},j,w}(T, p_w^{\sigma})$ denotes Henry's constant at the saturation pressure p_w^{σ} of the pure solvent, i.e., at infinite dilution of j . The lower integration limit in the Poynting correction has been approximately set to $p = 0$ MPa, as it was done by Sloan [35]. Like in our previous work [34], an average value of $V_{m,j}^{\infty,\text{L}_w} = 32 \text{ cm}^3 \text{ mol}^{-1}$ [51] was used for both gases. Henry's constant at T and p_w^{σ} was calculated from the empirical relation [35]

$$\frac{k_{\text{H},j,w}(T, p_w^{\sigma})}{1.01325 \times 10^5 \text{ Pa}} = \exp\left(-\frac{4.185 \text{ J}}{R \times \text{K mol}} \left(a_0 + a_1 \frac{\text{K}}{T} + a_2 \ln\left(\frac{T}{\text{K}}\right) + a_3 \frac{T}{\text{K}}\right)\right) \quad (6)$$

The numerical values of the constants a_0 , a_1 , a_2 and a_3 are listed in Table 2.

Table 2 Parameters appearing in the correlation (eq. (6)) for Henry's law constant

	a_0	a_1	a_2	a_3
CH_4^{a}	-365.183	18106.7	49.7554	-0.000285
CO_2^{a}	-317.658	17371.2	43.0607	-0.002191

^a 2nd ed. of the monograph of Sloan [35].

2.5 The eNRTL-model

For the case of a single solvent, aqueous multicomponent electrolyte system considered here, the eNRTL model [15,20] describes its molar excess Gibbs energy by referring to the basic microscopic characteristics of electrolyte solutions. The model accounts for the long ranging inter-ionic forces (subscript LR) and the short range forces (subscript SR) acting between the various species by splitting up the molar excess Gibbs energy $G_m^{\text{E}*}$ into the sum of the two corresponding contributions $G_{m,\text{LR}}^{\text{E}*}$ and $G_{m,\text{SR}}^{\text{E}*}$ [20], respectively, according to

$$G_m^{\text{E}*} = G_{m,\text{LR}}^{\text{E}*} + G_{m,\text{SR}}^{\text{E}*}, \quad (7)$$

where $G_{m,\text{LR}}^{\text{E}*}$ stands for the long-range and $G_{m,\text{SR}}^{\text{E}*}$ for the short-range contribution to $G_m^{\text{E}*}$. The asterisk denotes the unsymmetric reference state (see further below). From an expression for G_m^{E} or $G_m^{\text{E}*}$, expressions for the symmetrically referenced activity coefficients $\gamma_{x,j}$ and the unsymmetrically referenced activity coefficients $\gamma_{x,j}^*$ can be derived in the usual way via the thermodynamic relationships given in Appendix A.3. It follows from eq. (7) that for all species $j \in S_m \cup S_c \cup S_A$ (see explanations below) $\ln \gamma_{x,j}$ (as well as $\ln \gamma_{x,j}^*$) is given by

$$\ln \gamma_{x,j} = \ln \gamma_{x,j,\text{LR}} + \ln \gamma_{x,j,\text{SR}}, \quad (8)$$

where $\gamma_{x,j,\text{LR}}$ and $\gamma_{x,j,\text{SR}}$ are the respective contributions to $\gamma_{x,j}$. The presentation of the model in the following sub-sections is mainly based on the modification published by Bollas et al. [] of the multicomponent version of the eNRTL-model of Chen and Evans [

2.5.1 The description of the composition of the system

In the most general case the system is a multicomponent electrolyte solution consisting of N_m+1 molecular components m_0, m_1, \dots, m_{N_m} , N_C cationic species C_1, \dots, C_{N_C} and N_A anionic species A_1, \dots, A_{N_A} , respectively. Whereas m_0 stands for the molecular solvent (here water, i.e. $m_0 \equiv w$), m_1, \dots, m_{N_m} designates the set of possible additional molecular solute species, respectively. The corresponding sets of species are denoted by S_m , S_C and S_A , i.e.

$$\left. \begin{aligned} S_m &= \{m_0, m_1, \dots, m_{N_m}\} \\ S_C &= \{C_1, \dots, C_{N_C}\} \\ S_A &= \{A_1, \dots, A_{N_A}\} \end{aligned} \right\} \quad (9)$$

The systems treated here contain strong electrolytes $C_{\nu_{C,CA}} A_{\nu_{A,CA}}$ (abbreviated as CA) which dissociate completely into $\nu_{C,CA}$ cations C^{z_C+} and $\nu_{A,CA}$ anions $A^{|z_A| -}$



The composition of the system might either be characterised by means of the mole fraction x_j of species j , calculated from the complete set of mole numbers n_j of species according to

$$x_j = \frac{n_j}{\sum_{j' \in S_m \cup S_C \cup S_A} n_{j'}} \quad (\text{for all } j \in S_m \cup S_C \cup S_A), \quad (11)$$

or in terms of the amounts of the chemical components regardless of what happens to their particles when being dissolved. These quantities are called here “overall” or “apparent” quantities. For example, the overall molality \bar{b}_k of component k is defined as

$$\bar{b}_k = \frac{\bar{n}_k}{\bar{m}_w} = \frac{\bar{n}_k}{\bar{n}_w M_w} \quad (\text{for all } k \in \{S_m \cup S_{CA}\} \setminus \{w\}), \quad (12)$$

where \bar{n}_k is the overall mole number of component k , and \bar{m}_w and M_w are the overall mass and the molar mass of water, respectively. S_{CA} designates the set of salts used for preparing the respective solution, which in combination with the condition of complete dissociation determines unambiguously the mixture composition in terms its species.

2.5.2 The long-range interaction contribution

In the framework of the eNRTL model the long-range contribution to G_m^{E*} , $G_{m,\text{LR}}^{E*} = G_{m,\text{PDH}}^{E*}$, is modelled by a Debye-Hückel term as modified by Pitzer (indicated by subscript PDH), in which the solvent is treated as a dielectric continuum [17,18]. The set of independent variables for representing $G_{m,\text{PDH}}^{E*}$ consists of temperature, molar volume, the chemical potential of the solvent and the mole numbers of all solute species, corresponding to the so-called McMillan-Meyer-framework [52]. Therefore the Pitzer-Debye-Hückel equation is based on an unsymmetric reference state whereby $G_{m,\text{PDH}}^{E*}$ vanishes when the mole fraction of the solvent species x_w approaches unity.

$$\lim_{x_w \rightarrow 1} G_{m, \text{PDH}}^{\text{E}*} = 0, \quad (13)$$

$x_w \rightarrow 1$ is equivalent to the condition $\sum_{j \neq w} x_j \rightarrow 0$, explaining the term “unsymmetric”. $G_{m, \text{PDH}}^{\text{E}*}$ vanishes if the pure component state is approached for the solvent, but the state of infinite dilution is approached for the solute species.

Since $G_{m, \text{PDH}}^{\text{E}*}$ accounts for the long-range Coulomb forces between the charged species only, its composition dependence can be represented entirely by means of the ionic strength. The ionic strength, expressed with respect to the mole fraction concentration scale, I_x , is defined through the relation

$$I_x = \frac{1}{2} \sum_{j \in S_C \cup S_A} z_j^2 x_j \quad (14)$$

where z_j is the positive or negative charge number of ion j . With I_x , the defining equation for $G_{m, \text{PDH}}^{\text{E}*}$ [18] reads

$$\frac{G_{m, \text{LR}}^{\text{E}*}}{RT} = \frac{G_{m, \text{PDH}}^{\text{E}*}}{RT} = -4A_\phi M_w^{-1/2} \frac{I_x}{\rho} \ln(1 + \rho I_x^{1/2}) \quad (15)$$

In eq. (15), T denotes the absolute temperature, M_w the molar mass of the solvent water and ρ the closest approach parameter, respectively. A_ϕ is the so-called Debye-Hückel-parameter which for aqueous electrolyte systems can be expressed by

$$A_\phi = \frac{1}{3} \frac{(2N_{\text{Av}} \rho_w^\circ)^{1/2}}{8\pi} \left(\frac{e^2}{\epsilon_0 \epsilon_{r, w}^\circ k_B T} \right)^{3/2}, \quad (16)$$

where N_{Av} , k_B , e , and ϵ_0 stands for the Avogadro constant, the Boltzmann constant, the elementary charge and the permittivity of free space, respectively [41]. $\epsilon_{r, w}^\circ$ is the relative permittivity and ρ_w° the density of water, respectively. Since the numerical value for each of the quantities in eq. (15) and (16) depends on the respective unit employed, the numerical factor 1000 given in the original publications (e.g. [17,18,53]) has been omitted in both eq. (15) and eq. (16). A_ϕ is based on molality as the underlying composition scale and has the dimension $\text{mass}^{1/2} \times (\text{amount of substance})^{-1/2}$. Numerical values of the Debye-Hückel parameter are usually given in $\text{kg}^{1/2} \text{mol}^{-1/2}$ and at 298.15 K $A_\phi = 0.391 \text{kg}^{1/2} \text{mol}^{-1/2}$. In case of water being the solvent, A_ϕ is provided as an empirical function of temperature by Chen et al. [20], which was also used here. It should be remarked that the expression given in [20] has to be multiplied by $\text{kg}^{1/2} \text{mol}^{-1/2}$ to give the correct results. The closest approach parameter ρ has been set to a value of 14.9 in accordance with the work of Chen and co-workers [20,21].

The general expression for the long range interaction contribution to the activity coefficient $\gamma_{x, j, \text{LR}}^*$, valid for all types of species, ionic as well as molecular solute and solvent species, i.e., $j \in S_m \cup S_C \cup S_A$, is derived from eq. (15) by using eq. (A.8) in appendix A.3.

$$\ln \gamma_{x, j, \text{LR}}^* = -A_\phi M_w^{-1/2} \left(\left(\frac{2z_j^2}{\rho} \right) \ln(1 + \rho I_x^{1/2}) + \frac{z_j^2 I_x^{1/2} - 2 I_x^{3/2}}{1 + \rho I_x^{1/2}} \right) \quad (17)$$

2.5.3 The short-range interaction contribution

A modified version of the Non-Random-Two-Liquid model of Renon and Prausnitz [54] (indicated by subscript mod-NRTL) which is based on the local composition concept (index

LC) is used to describe the short range contribution $G_{m,SR}^{E*} = G_{m,mod-NRTL}^{E*} = G_{m,LC}^{E*}$ to G_m^{E*} . In contrast to the Pitzer-Debye-Hückel model, the modified NRTL model is based on a symmetric reference state, i.e., it provides an expression for $G_{m,SR}^E$, the symmetrically referenced molar excess Gibbs energy rather than for $G_{m,SR}^{E*}$. In other words, the model uses the pure liquid solvent, the hypothetically pure liquid molecular and the hypothetically pure liquid homogeneously mixed electrolyte solutes, respectively, as reference states.

$$\left. \begin{aligned} \lim_{\bar{x}_w \rightarrow 1} G_{m,SR}^E &= 0 \\ \lim_{\bar{x}_m \rightarrow 1} G_{m,SR}^E &= 0 \quad (\text{for all } m \in S_m \setminus \{w\}) \\ \lim_{\bar{x}_{CA} \rightarrow 1} G_{m,SR}^E &= 0 \quad (\text{for all } CA \in S_{CA}) \end{aligned} \right\} \quad (18)$$

where \bar{x}_w , \bar{x}_m and \bar{x}_{CA} denote the overall mole fractions of the solvent, the molecular and the electrolyte solute components, respectively.

The reference value used for defining the short range contribution to the excess molar Gibbs energy is the residual molar Gibbs energy of the pure molecular component/species for each $m \in S_m$. The hypothetically homogeneously mixed completely dissociated liquid electrolyte mixture [21] is used as reference state for the residual molar Gibbs energy of ionic species $C \in S_C$ and $A \in S_A$ respectively.

$$G_{m,m-cell}^{R \text{ ref}} = G_{m,m-cell}^{R \circ} = g_{mm} \quad (\text{for all } m \in S_m) \quad (19)$$

$$G_{m,C-cell}^{R \text{ ref}} = z_C \sum_{A \in S_A} Y_A g_{AC} \quad (\text{for all } C \in S_C) \quad (20)$$

$$G_{m,A-cell}^{R \text{ ref}} = |z_A| \sum_{C \in S_C} Y_C g_{CA} \quad (\text{for all } A \in S_A) \quad (21)$$

In eqs. (19)-(21), g_{mm} , g_{AC} and g_{CA} denote the energies of interaction between m - m , A - C and C - A species, respectively. With regard to the individual ionic activity coefficients, the symmetrical reference frame implies that the activity coefficients approach unity only if for a given $C \in S_C$ (or $A \in S_A$) all other ions vanish except for another single counter ion $A \in S_A$ (or $C \in S_C$). This corresponds to the state of the pure, hypothetically homogeneously mixed liquid pure electrolyte component CA . In eqs. (20) and (21), Y_A and Y_C are the so-called ionic charge fractions defined according to [15]

$$Y_C = \frac{X_C}{\sum_{C' \in S_C} X_{C'}} \quad (\text{for all } C \in S_C) \quad (22)$$

$$Y_A = \frac{X_A}{\sum_{A' \in S_A} X_{A'}} \quad (\text{for all } A \in S_A) \quad (23)$$

In eqs. (22) and (23), X_j is the effective mole fraction of species j which is defined by [21]

$$X_j = x_j c_j \quad \text{with } c_j = \begin{cases} 1 & \text{for } j \in S_m \\ |z_j| & \text{for } j \in S_C \cup S_A \end{cases} \quad (24)$$

The symmetric reference frame leads to the following expression for $G_{m,SR}^E$ [21]

$$\begin{aligned}
\frac{G_{m,SR}^E}{RT} = & \sum_{m \in S_m} X_m \frac{\sum_{j \in S_m \cup S_C \cup S_A} X_j G_{jm} \tau_{jm}}{\sum_{j' \in S_m \cup S_C \cup S_A} X_{j'} G_{j'm}} + \sum_{C \in S_C} X_C \sum_{A \in S_A} Y_A \frac{\sum_{j \in S_m \cup S_A} X_j G_{jC,AC} \tau_{jC,AC}}{\sum_{j' \in S_m \cup S_A} X_{j'} G_{j'C,AC}} \\
& + \sum_{A \in S_A} X_A \sum_{C \in S_C} Y_C \frac{\sum_{j \in S_m \cup S_C} X_j G_{jA,CA} \tau_{jA,CA}}{\sum_{j' \in S_m \cup S_C} X_{j'} G_{j'A,CA}}
\end{aligned} \quad (25)$$

where G_{jm} , $G_{jC,AC}$ and $G_{jA,CA}$ are the Boltzmann kind factors and τ_{jm} , $\tau_{jC,AC}$ and $\tau_{jA,CA}$ the corresponding dimensionless interaction energy parameters [15,21]. The quantities G_{jm} for $j = m'$, C and A, respectively, are calculated for any $m \in S_m$ according to [15,21]

$$G_{m'm} = \exp(-\alpha_{m'm} \tau_{m'm}) \quad (\text{for all } m' \in S_m, m \in S_m) \quad (26)$$

$$G_{Cm} = \sum_{A \in S_A} Y_A G_{CA,m} \quad (\text{for all } C \in S_C, m \in S_m) \quad (27)$$

$$G_{Am} = \sum_{C \in S_C} Y_C G_{CA,m} \quad (\text{for all } A \in S_A, m \in S_m) \quad (28)$$

$G_{CA,m}$ in turn is given by [55]

$$G_{CA,m} = \exp(-\alpha_{CA,m} \tau_{CA,m}) \quad (\text{for all } m \in S_m, C \in S_C, A \in S_A), \quad (29)$$

where $\alpha_{CA,m}$ and $\tau_{CA,m}$ are basic model parameters. The Boltzmann kind factors $G_{jC,AC}$ for $j = m, A'$, and $G_{jA,CA}$ for $j = m, C'$, are defined similarly to eq. (26) and eq. (29) [55] by

$$G_{jC,AC} = \exp(-\alpha_{jC,AC} \tau_{jC,AC}) \quad (\text{for all } j \in S_m \cup S_A, C \in S_C, A \in S_A) \quad (30)$$

$$G_{jA,CA} = \exp(-\alpha_{jA,CA} \tau_{jA,CA}) \quad (\text{for all } j \in S_m \cup S_C, C \in S_C, A \in S_A) \quad (31)$$

In eqs. (26) and (29-31), the dimensionless quantities $\alpha_{m'm}$, $\alpha_{jC,AC}$ and $\alpha_{jA,CA}$ are the so-called nonrandomness factors.

The interaction energy parameters τ_{Cm} and τ_{Am} are obtained from [15]

$$\tau_{Cm} = -\frac{\ln G_{Cm}}{\alpha_{Cm}} \quad (\text{for all } C \in S_C, m \in S_m) \quad (32)$$

$$\tau_{Am} = -\frac{\ln G_{Am}}{\alpha_{Am}} \quad (\text{for all } A \in S_A, m \in S_m) \quad (33)$$

where the α_{jm} 's are obtained from the independent nonrandomness factors $\alpha_{CA,m} \equiv \alpha_{m,CA}$ via the same type of mixing rule as the one being used for calculating the quantity G_{jm} [15,21].

$$\alpha_{Cm} = \sum_{A \in S_A} Y_A \alpha_{CA,m} \quad (\text{for all } C \in S_C, m \in S_m) \quad (34)$$

$$\alpha_{Am} = \sum_{C \in S_C} Y_C \alpha_{CA,m} \quad (\text{for all } A \in S_A, m \in S_m) \quad (35)$$

Whereas $\alpha_{A'C,AC} \equiv \alpha_{AC,A'C}$ and $\alpha_{C'A,CA} \equiv \alpha_{CA,C'A}$ as well as $\tau_{A'C,AC}$, $\tau_{AC,A'C}$, $\tau_{C'A,CA}$ and $\tau_{CA,C'A}$ belong to the set of basic parameters of the model, $\tau_{mC,AC}$ and $\tau_{mA,CA}$ are composition dependent quantities which are derived by means of the following relations [15,23]

$$\tau_{mC,AC} = \tau_{Cm} - \frac{\alpha_{CA,m}}{\alpha_{mC,AC}} (\tau_{CA,m} - \tau_{m,CA}) \quad (\text{for all } m \in S_m, C \in S_C, A \in S_A) \quad (36)$$

$$\tau_{mA,CA} = \tau_{Am} - \frac{\alpha_{CA,m}}{\alpha_{mA,CA}} (\tau_{CA,m} - \tau_{m,CA}) \quad (\text{for all } m \in S_m, C \in S_C, A \in S_A) \quad (37)$$

Like $\tau_{m'm}$ and $\tau_{CA,m}$, $\tau_{m,CA}$ is yet another independent model parameter. In contrast, $\alpha_{mC,AC}$ and $\alpha_{mA,CA}$ are set to [15,23]

$$\alpha_{mC,AC} = \alpha_{Cm} \quad (\text{for all } m \in S_m, C \in S_C, A \in S_A) \quad (38)$$

$$\alpha_{mA,CA} = \alpha_{Am} \quad (\text{for all } m \in S_m, C \in S_C, A \in S_A) \quad (39)$$

Since the solvent activity coefficient, $\gamma_{x,w}^{L_w}$, is of fundamental importance in modelling the H-L_w-G-equilibria treated in this study, the expression for the short range contribution to the symmetrically referenced activity coefficient $\gamma_{x,m,SR}$ of molecular species m is explicitly presented at this stage. Partial differentiation of the $G_{m,SR}^E$ -expression defined in eq. (25) with respect to n_j for $j = m$ ($m \in S_m$) according to eq. (A.8) leads to the equation for $\ln \gamma_{x,m,SR}$

$$\begin{aligned} \ln \gamma_{x,m,SR} = & \frac{\sum_{j \in S_m \cup S_C \cup S_A} X_j G_{jm} \tau_{jm}}{\sum_{j' \in S_m \cup S_C \cup S_A} X_{j'} G_{j'm}} + \sum_{m' \in S_m} \frac{X_{m'} G_{mm'}}{\sum_{j' \in S_m \cup S_C \cup S_A} X_{j'} G_{j'm'}} \left(\tau_{mm'} - \frac{\sum_{j \in S_m \cup S_C \cup S_A} X_j G_{jm'} \tau_{jm'}}{\sum_{j' \in S_m \cup S_C \cup S_A} X_{j'} G_{j'm'}} \right) \\ & + \sum_{C \in S_C} \sum_{A' \in S_A} \frac{Y_{A'} X_C G_{mC,A'C}}{\sum_{j' \in S_m \cup S_A} X_{j'} G_{j'C,A'C}} \left(\tau_{mC,A'C} - \frac{\sum_{j \in S_m \cup S_A} X_j G_{jC,A'C} \tau_{jC,A'C}}{\sum_{j' \in S_m \cup S_A} X_{j'} G_{j'C,A'C}} \right) \\ & + \sum_{A \in S_A} \sum_{C' \in S_C} \frac{Y_{C'} X_A G_{mA,C'A}}{\sum_{j' \in S_m \cup S_C} X_{j'} G_{j'A,C'A}} \left(\tau_{mA,C'A} - \frac{\sum_{j \in S_m \cup S_C} X_j G_{jA,C'A} \tau_{jA,C'A}}{\sum_{j' \in S_m \cup S_C} X_{j'} G_{j'A,C'A}} \right) \end{aligned} \quad (40)$$

Eq. (40) holds for all $m \in S_m$ and thus also for $m = m_0 \equiv w$. Since $\gamma_{x,w,SR}$ is normalised in line with the unsymmetric convention according to the pure component reference frame, no further adjustment of the value derived from eq. (38) is needed for this case. Contrary, for deriving the activity coefficients of molecular solute species $m \in S_m \setminus \{w\}$, which in accordance with the unsymmetric convention are usually expressed within the Henry's law reference frame, normalisation of the activity coefficient to the infinite dilute state is required for obtaining $\ln \gamma_{x,m,SR}^*$. Even though the presence of molecular solutes dissolved in the liquid phase was neglected in this work, the corresponding formula for $\ln \gamma_{x,m,SR}^\infty$ [15], derived by means of eq. (A.3), is mentioned here for the sake of completeness.

$$\ln \gamma_{x,m,SR}^\infty = \tau_{wm} + G_{mw} \tau_{mw} \quad (\text{for all } m \in S_m \setminus \{w\}) \quad (41)$$

In contrast to $\gamma_{x,w,SR}$, the expressions for the activity coefficients of the ionic species are not required for the exclusive modelling of the incipient gas hydrate formation conditions. Nevertheless, they are also discussed in the framework of this study for two reasons (see

appendix A.4): Firstly since $\ln \gamma_{x,j}$ (along with $\ln \gamma_{x,j}^*$, the mean ionic activity coefficients $\ln \gamma_{x,CA,\pm}^*$ and $\ln \gamma_{m,CA,\pm}^*$, as well as the infinite dilution activity coefficients $\ln \gamma_{x,j}^\infty$) for all $j \in S_C \cup S_A$, as given in both eNRTL model versions [21,23] were also incorporated in the model implementation of this work. Secondly, since the most general expression for $\ln \gamma_{x,C,SR}$ in the refined eNRTL-model [23] does contain a typing error, while the expressions for both, $\ln \gamma_{x,C,SR}^\infty$ and $\ln \gamma_{x,A,SR}^\infty$ presented in [23], respectively, are erroneous.

2.5.4 On the basic model parameters and their temperature dependence

The basic model parameters to be adjusted to binary {water + electrolyte} systems at constant temperature are the nonrandomness factor $\alpha_{w,CA}$ and the dimensionless energetic interaction parameters $\tau_{w,CA}$ and $\tau_{CA,w}$. The latter are weak but well behaved functions of temperature. In practice, the nonrandomness factor is often a priori set to a fixed value. Hence, only two parameters are needed to describe an isothermal solution of a single electrolyte [21]. For the general case of a multicomponent system under isothermal conditions, containing besides the solvent additional molecular solutes as well as ionic species, combinatorial considerations lead to the number of eNRTL model parameters required for its description (Appendix A.5).

In multicomponent systems the independent model parameters are $\alpha_{mm'}$, $\alpha_{m,CA}$, $\alpha_{CA,CA'}$, $\alpha_{AC,AC'}$, $\tau_{mm'}$, $\tau_{m'm}$, $\tau_{m,CA}$, $\tau_{CA,m}$, $\tau_{AC,AC'}$, $\tau_{AC',AC}$, $\tau_{CA,CA'}$, and $\tau_{CA',CA}$. $\tau_{mm'}$, $\tau_{m'm}$ (and possibly $\alpha_{mm'}$) are adjusted to molecule-molecule binary systems (these values can be taken from data sources for the NRTL-model). $\tau_{AC,AC'}$, $\tau_{AC',AC}$, $\tau_{CA,CA'}$, and $\tau_{CA',CA}$ (and possibly $\alpha_{CA,CA'}$ and $\alpha_{AC,AC'}$) are adjusted to ternary {solvent + salt₁ + salt₂} systems involving electrolytes having one ion in common. Actually it can be set $\tau_{AC,AC'} = -\tau_{AC',AC}$ and $\tau_{CA,CA'} = -\tau_{CA',CA}$ [21]. Good results are even obtained by setting these parameters to zero [21]. This is an example for demonstrating the predictive capabilities of the model.

The non-randomness parameters are usually set to default values, as it was also done in this work. Whereas $\alpha_{mm'} = 0.3$ is typically used for describing the molecule-molecule interactions (parameter was not used in these calculations since no molecule-molecule interaction was taken into account), a value of 0.2 is usually adopted for $\alpha_{m,CA}$, $\alpha_{CA,CA'}$ and $\alpha_{AC,AC'}$ [53]. Confining to this procedure, $\alpha_{m,CA}$ was set to 0.2 throughout in this study.

The parameters $\tau_{mm'}$, $\tau_{m,CA}$, $\tau_{CA,m}$, $\tau_{CA,C'A}$ and $\tau_{AC,A'C}$, respectively, are functions of temperature. Their dependence on temperature is described by means of empirical functions. The molecule-molecule interaction parameters are described by [53]

$$\tau_{mm'}(T) = A_{mm',0} + \frac{A_{mm',1}}{T} + A_{mm',2} \ln\left(\frac{T}{K}\right) + A_{mm',3}T \quad (42)$$

whereas the following functions are proposed for describing $\tau_{m,CA}(T)$ and $\tau_{CA,m}(T)$

$$\tau_{m,CA}(T) = B_{m,CA,0} + \frac{B_{m,CA,1}}{T} + B_{m,CA,2} \left(\frac{T - T^{\text{ref}}}{T} + \ln\left(\frac{T}{T^{\text{ref}}}\right) \right), \quad (43)$$

$$\tau_{CA,m}(T) = B_{CA,m,0} + \frac{B_{CA,m,1}}{T} + B_{CA,m,2} \left(\frac{T - T^{\text{ref}}}{T} + \ln\left(\frac{T}{T^{\text{ref}}}\right) \right), \quad (44)$$

Similarly, $\tau_{CA,C'A}(T)$ and $\tau_{AC,A'C}(T)$ are modelled by

$$\tau_{CA,C'A}(T) = B_{CA,C'A,0} + \frac{B_{CA,C'A,1}}{T} + B_{CA,C'A,2} \left(\frac{T - T^{\text{ref}}}{T} + \ln \left(\frac{T}{T^{\text{ref}}} \right) \right) \quad (45)$$

$$\tau_{AC,A'C}(T) = B_{AC,A'C,0} + \frac{B_{AC,A'C,1}}{T} + B_{AC,A'C,2} \left(\frac{T - T^{\text{ref}}}{T} + \ln \left(\frac{T}{T^{\text{ref}}} \right) \right) \quad (46)$$

In the expressions for $\tau_{CA,C'A}(T)$ and $\tau_{AC,A'C}(T)$, the values for $B_{CA,C'A,0}$, $B_{CA,C'A,1}$ and $B_{CA,C'A,2}$, and $B_{AC,A'C,0}$, $B_{AC,A'C,1}$ and $B_{AC,A'C,2}$, respectively, are often set to zero, like it was also done in this study. T^{ref} is set to 298.15 K [53].

2.6 The thermodynamic description of the gas phase

An equation of state (EOS) approach was used to describe the vapour phase throughout in the calculations while a cubic equation of state, the Soave-Redlich-Kwong (SRK) EOS [42], served for calculating the fugacities of the gaseous components in the gas phase. The presence of water in the gas phase was neglected, i.e., it was assumed that $f_{\text{H}_2\text{O}}^G = 0$. Like in our previous work [34], the values for the SRK-EOS-parameters were taken from Danesh [56].

2.7 Details on the eNRTL model implementation and overall modelling procedure

The modelling of the incipient hydrate forming conditions in systems comprising one of the guest components CH_4 or CO_2 and an aqueous solution of one or two strong electrolytes was performed by means of our updated in-house programme mentioned earlier. As the main part of this work, both the previous version of the eNRTL model by Chen and Evans [21] as well as the more recent version of the model by Bollas et al. [23] were incorporated into the previous programme designed for gas hydrate modelling of systems without electrolytes. The newly implemented eNRTL routines (called “classes” in the object oriented Java language) provide expressions for treating multicomponent systems composed of the solvent water and any number of molecular, cationic and anionic solute species. Mixed solvent systems as included through the model extension of Mock et al. [57] were thus not taken into account. In particular, the eNRTL implementation contains functions (called “methods” in Java) for the calculation of individual ionic and molecular species’ activity coefficients, mean ionic activity coefficients, both with respect to the mole fraction and molality concentration scale, and the osmotic coefficient, respectively. Expressions for the different types of activity coefficients at infinite dilution were also provided. The unsymmetric convention was adopted for normalising the activity coefficients, i.e., the Henry’s law reference frame was used for the solute species, whereas the Lewis-Randall reference frame was applied in case of the solvent species. The basic eNRTL model parameters used for representing the energetic interaction parameters as function of temperature were retrieved from the Aspen Properties[®] data bank and provided to the programme by means of an xml-data file.

The algorithm presented by Sloan [35] was used for calculating the incipient hydrate formation conditions at H-L_w-G-phase equilibrium. Its central element is the solution of eq. (1) for the unknown state variables. In calculating the activity of water, the influence of the dissolved gases on the liquid phase non-idealities was neglected. The mole fraction of the gas dissolved in the liquid phase was thus estimated by means of the Henry’s law approach presented in section 2.4 by assuming that $\gamma_{x,\text{CH}_4}^{*,L_w} = \gamma_{x,\text{CO}_2}^{*,L_w} = 1$. In the calculation of $\gamma_{x,w}^{*,L_w}$, the influence of the dissolved gases on $\gamma_{x,w}^{*,L_w}$ was neglected by setting $\tau_{w,j} = \tau_{j,w} = 0$ ($j = \text{CH}_4, \text{CO}_2$). The gas-salt-interaction parameters were also set to zero. With regard to the Kihara parameters σ_{jw} and ε_{jw} ($j = \text{CH}_4, \text{CO}_2$) it turned out that it was sufficient to use the

set of values obtained in our previous study [34] to achieve a good overall description of the incipient hydrate formation conditions at fixed salt concentration in the initial solutions.

3 Modelling Results and Discussion

3.1 Verification of the correctness of the eNRTL model implementation

Initially, in view of the quite lengthy multicomponent eNRTL-expressions for the activity coefficients, the correctness of the model implementation was thoroughly examined. For that purpose, calculated results of numerous selected examples were compared to corresponding experimental data. Mean molal activity coefficients, osmotic coefficients and solubilities were investigated for single and mixed aqueous electrolyte solutions.

3.1.1 Osmotic coefficient of binary {solvent + salt} systems

The calculations carried out for checking the correctness of the code were inspired by the systems treated in the publication of Chen and Evans [21]. In the first examples the osmotic coefficient ϕ was modelled at 25 °C and ambient pressure for single salt aqueous solutions of alkali metal chlorides MCl (M = Li, Na, K, Rb) and alkaline earth metal halides MX₂ (M = Mg, Ca; X = Cl, Br, I), respectively, using data for the solvent-salt interaction coefficients reported in [21]. The quantity ϕ is derived by means of eq. (A.13) using calculated results for $\gamma_{x,w}$. eNRTL-model parameters were taken from [21]

Root mean square relative deviations between the calculated results and the experimental data of Robinson and Stokes [58], defined according to

$$\sigma_{\phi, \text{rel}} = \sqrt{\frac{1}{N_{\text{exp data}}} \sum_{q=1}^{N_{\text{exp data}}} \left(\frac{\phi_{\text{exp}, q} - \phi_{\text{calc}, q}}{\phi_{\text{exp}, q}} \right)^2} \quad (47)$$

are compiled in Table 3. As can be verified in Table 3, the values of $\sigma_{\phi, \text{rel}}$ generated in this work reproduce the corresponding $\sigma_{\phi, \text{rel}}$ -values of Chen and Evans [21].

Table 3 Comparison of values for the root mean square deviation $\sigma_{\phi, \text{rel}}$ between calculated and experimental results [58] on the osmotic coefficient at 25 °C and ambient pressure obtained in this study and by Chen and Evans [21], respectively, for selected alkali chloride and alkaline earth metal halide aqueous solutions

Salt	$\sigma_{\phi, \text{rel}}^a$	$\sigma_{\phi, \text{rel}}^b$	$\bar{b}_{\text{CA}, \text{max}}$
LiCl	0.0227	0.024	6
NaCl	0.0118	0.012	6
KCl	0.0023	0.002	4.8
RbCl	0.0015	0.002	5
CaCl ₂	0.0238	0.025	2.5
CaBr ₂	0.1235	0.13	6
CaI ₂	0.0220	0.024	2
MgCl ₂	0.0838	0.09	5
MgBr ₂	0.0896	0.09	5
MgI ₂	0.1036	0.11	5

^a This work.

3.1.2 Ternary {solvent + salt₁ + salt₂} systems

Calculations on solvent + salt₁ + salt₂ systems were performed in order to provide evidence for the correctness of the programme implementation for the general case of multicomponent electrolyte solutions. In each of these selected systems, the two different salts have one of their ions in common, i.e., they are either of the type {H₂O + C₁A + C₂A} or {H₂O + CA₁ + CA₂}. Osmotic coefficients ϕ , mean molal activity coefficients $\gamma_{b,\pm,CA}^*$ and salt solubilities were derived and compared to results found in the literature.

At first, in an attempt to reproduce Figure 2 given in [21], ϕ was calculated for the system {H₂O + NaCl + LiCl} at $T = 298.15$ K, $p = 0.1$ MPa and constant overall electrolyte molality of $\bar{b}_{\text{NaCl+LiCl}} = 2 \text{ mol kg}^{-1}$ as function of the relative amount of LiCl in the salt mixture (Figure 1). The latter was expressed in terms of the overall mole fraction of LiCl in the solvent-free binary sub-system {NaCl + LiCl}, i.e., $\bar{x}_{\text{LiCl, NaCl+LiCl}} = \bar{b}_{\text{LiCl}} / (\bar{b}_{\text{NaCl}} + \bar{b}_{\text{LiCl}})$. ϕ was modelled for three different values of the salt-salt-interaction parameters. Chen and Evans claimed that the curves B, C, and D in Figure 2 of their article [21] would correspond to parameter values of $\tau_{\text{Na}^+\text{Cl}^-, \text{Li}^+\text{Cl}^-} = -\tau_{\text{Li}^+\text{Cl}^-, \text{Na}^+\text{Cl}^-} = 0, 1$ and 2 and $\alpha = 0.2$. The curves B-D given in Figure 2 of the original publication along with the linear interpolation line A between $\phi(\bar{x}_{\text{LiCl, NaCl+LiCl}} = 0)$ and $\phi(\bar{x}_{\text{LiCl, NaCl+LiCl}} = 1)$ are reproduced from [21] by means of the programme “plotdigitizer” provided by the Physics Department of the University of South Alabama, USA [59]. They are represented as red lines in Figure 1 a) and b). Although Chen and Evans do not explicitly mention the numerical values $\tau_{\text{CA,w}}$ and $\tau_{\text{w,CA}}$ used for creating the curves of ϕ against $\bar{x}_{\text{LiCl, NaCl+LiCl}}$ it can be assumed that they used the data presented in Table 1 of the same publication [21]. The latter are compiled in the rows labelled as “Figure 1 a)” in Table 4. Using these values for $\tau_{\text{CA,w}}$ and $\tau_{\text{w,CA}}$, and 0, 1, 2 for the salt-salt parameters, the curves published in [21] could not be reproduced. However, when incrementing the values of the latter by one, and hence setting $\tau_{\text{Na}^+\text{Cl}^-, \text{Li}^+\text{Cl}^-} = -\tau_{\text{Li}^+\text{Cl}^-, \text{Na}^+\text{Cl}^-} = 1, 2, 3$, the curves B-D could at least be reproduced qualitatively (see light blue curves of Figure 1 a)). Nevertheless, the values of $\phi(\bar{x}_{\text{LiCl, NaCl+LiCl}} = 0)$ between this work and [21] do still not match. Using for $\tau_{\text{CA,w}}$ and $\tau_{\text{w,CA}}$ the values provided by Chen et al. [20] and listed in the last two rows of Table 4 again together with $\tau_{\text{Na}^+\text{Cl}^-, \text{Li}^+\text{Cl}^-} = -\tau_{\text{Li}^+\text{Cl}^-, \text{Na}^+\text{Cl}^-} = 1, 2, 3$ results in the turquoise curves in Figure 1 b). Although the values of $\phi(\bar{x}_{\text{LiCl, NaCl+LiCl}} = 0)$ do almost coincide, a deviation can be detected for $\phi(\bar{x}_{\text{LiCl, NaCl+LiCl}} = 1)$ between this work and [21].

Since the correctness of the Java implementation has been checked independently through the same calculations performed by using the computer algebra software Mathcad[®] (version 14), it is believed that the results calculated in this work are correct. This conclusion is additionally supported by the fact that the change in slope of the curve D generated in this work (light blue and turquoise curve D in Figure 1 a) and b)) is smoother than it is for the corresponding curve presented by Chen and Evans (red curve D).

Table 4 Binary water-salt interaction coefficients used for generating the light blue and turquoise curves in Figure 1 a) and b), respectively, of ϕ for {H₂O + NaCl + LiCl}

	CA	$\tau_{\text{w,CA}}$	$\tau_{\text{CA,w}}$
Figure 1 a) ^a	NaCl	9.0234	-4.5916
	LiCl	10.1242	-5.1737

Figure 1 b) ^b	NaCl	8.885	-4.549
	LiCl	10.031	-5.154

^a Chen and Evans [21].

^b Chen et al. [20].

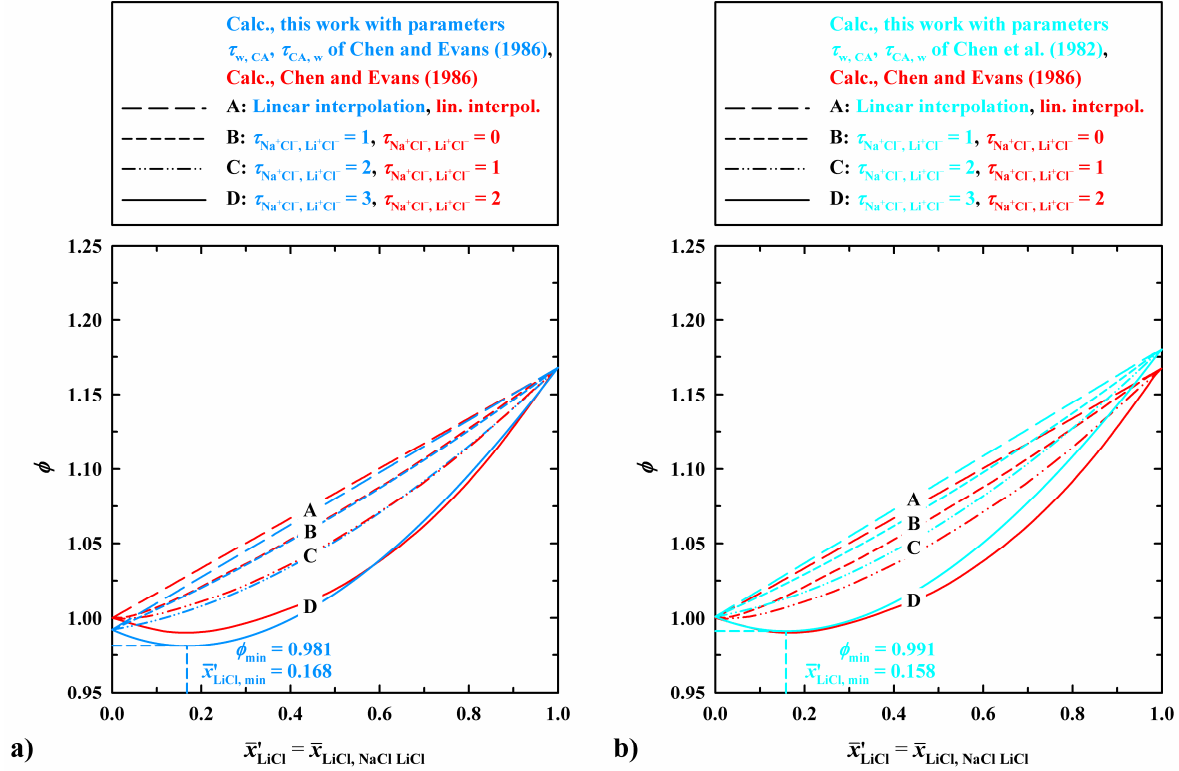


Figure 1 Osmotic coefficient of the system $\{H_2O + NaCl + LiCl\}$ at constant total overall molality $\bar{b}_{NaCl+LiCl} = 2 \text{ mol kg}^{-1}$, $T = 298.15 \text{ K}$ and ambient pressure as function of the salt mole fraction $\bar{x}_{LiCl, NaCl+LiCl} = \bar{b}_{LiCl} / (\bar{b}_{NaCl} + \bar{b}_{LiCl})$. Light blue curves in a) and turquoise curves in b), this work with solvent-salt parameters given in [21] and [20], respectively, and salt-salt-parameters $\tau_{NaCl, LiCl} = -\tau_{LiCl, NaCl} = 1, 2, 3$ for curves B-D, respectively. Red curves in a) and b) reproductions of the curves presented in Figure 2 of the original publication of Chen and Evans [21] with supposed values $\tau_{NaCl, LiCl} = -\tau_{LiCl, NaCl} = 0, 1, 2$. Curves A: linear interpolation.

As a further example for verifying the correctness of our eNRTL model implementation, the mean molal activity coefficients $\gamma_{b, CA, \pm}^*$ of NaCl and KCl in the $\{H_2O + NaCl + KCl\}$ -system have been modelled at 25°C (Figure 2) using eqs. (A.9)-(A.12) along with eqs. (A.15)-(A.18). For the expressions for $\gamma_{x, j}$ and $\gamma_{x, j}^\infty$ ($j \in S_C \cup S_A$) in the older model version, the reader is referred to [21] and [15], respectively. The calculations were inspired by Figure 1 presented in the article of Bollas et al. [23] in which the authors have performed calculations on $\gamma_{b, NaCl, \pm}^*$ and $\gamma_{b, KCl, \pm}^*$ using values for the salt-salt-interaction parameters of $\tau_{Na^+Cl^-, K^+Cl^-} = -\tau_{K^+Cl^-, Na^+Cl^-} = 0, 0.25, 0.50$ to compare the performance of the simplified [21] (Figure 2 a)) and the refined eNRTL model version (Figure 2 b)), respectively [23]. The reproducibility of the curves given in [23] (reproduced from [23] as red and orange lines in Figure 2, respectively, using the freely available programme “plotdigitizer” [59]) by means of our

programme in both model versions (blue and turquoise lines in Figure 2, respectively) serves as a further evidence that both the new [23] and the previous model equations [21] had been correctly implemented in our programme.

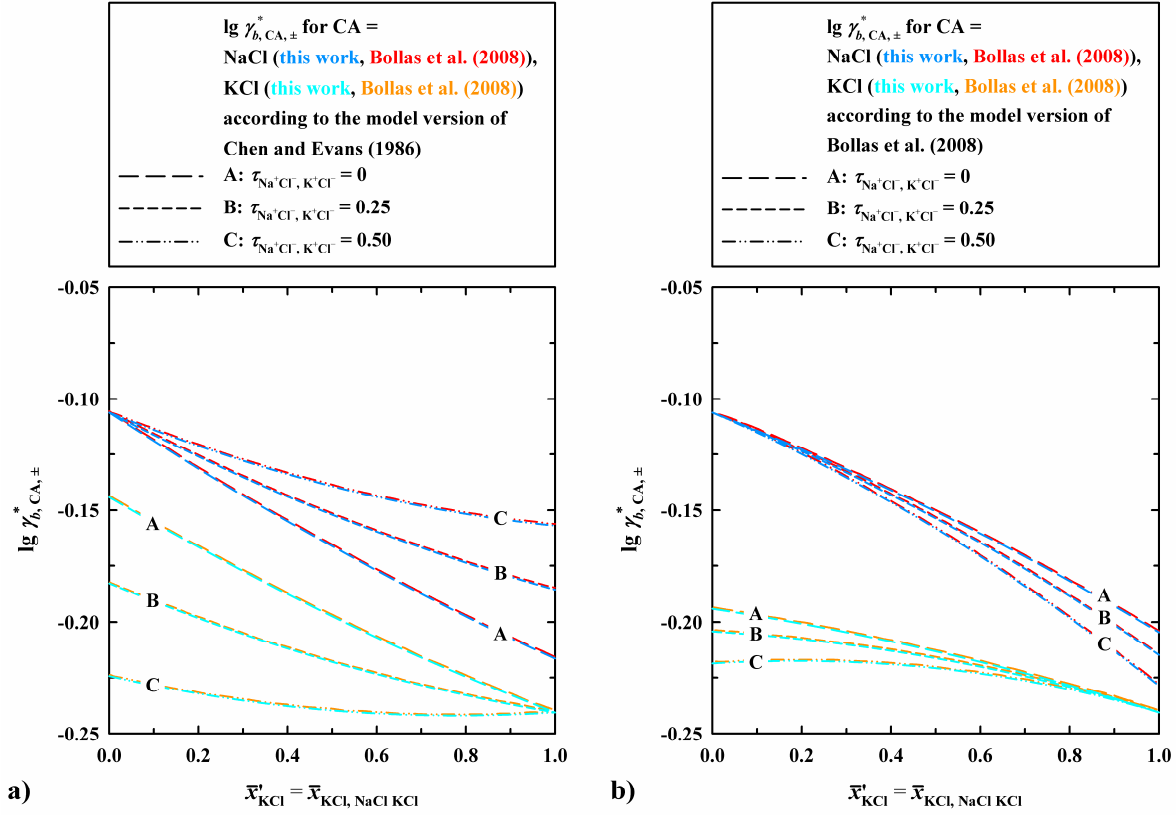


Figure 2 Prediction of the mean molal ionic activity coefficients of NaCl and KCl, $\gamma_{b, \text{NaCl}, \pm}^*$ and $\gamma_{b, \text{KCl}, \pm}^*$, of the system $\{\text{H}_2\text{O} + \text{NaCl} + \text{KCl}\}$ at 298.15 K and a total overall molality $b_{\text{NaCl} + \text{KCl}} = 4 \text{ mol kg}^{-1}$ with various salt-salt energy parameters using the equations for $\gamma_{x, \text{C}}^*$ and $\gamma_{x, \text{A}}^*$ of a) Chen and Evans [21] and b) Bollas et al. [23]. Comparison between the results of the eNRTL implementation for $\gamma_{b, \text{NaCl}, \pm}^*$ and $\gamma_{b, \text{KCl}, \pm}^*$ in this work and the results on $\gamma_{b, \text{NaCl}, \pm}^*$ and $\gamma_{b, \text{KCl}, \pm}^*$ given in [23].

3.1.3 $\text{S}_{\text{KX-L}_w}$ and $\text{S}_{\text{KCl-S}_{\text{KI-L}_w}}$ equilibria encountered in the system $\{\text{H}_2\text{O} + \text{KI} + \text{KCl}\}$

As an example for equilibrium calculations performed with the eNRTL model, the solubility curve of the system $\{\text{H}_2\text{O} + \text{KI} + \text{KCl}\}$ at $T = 298.15 \text{ K}$ and $p = 0.1 \text{ MPa}$ is shown in Figure 3. To model the solubilities in this ternary electrolyte system, values for the solubility products of the salts, $K_{\text{sp, KI}}$ and $K_{\text{sp, KCl}}$, are needed in addition to the eNRTL model parameters. With $K_{\text{sp, KI}} = -4.2346$ and $K_{\text{sp, KCl}} = -5.9695$ [21] gained from a data regression of the solubility data of Linke [60], the salt-solvent interaction parameters $\tau_{\text{K}^+\text{I}^-, \text{w}} = -4.1217$, $\tau_{\text{w}, \text{K}^+\text{I}^-} = 7.9408$, $\tau_{\text{K}^+\text{Cl}^-, \text{w}} = -4.1341$ and $\tau_{\text{w}, \text{K}^+\text{Cl}^-} = 8.1354$ [21] and the salt-salt-parameters $\tau_{\text{K}^+\text{Cl}^-, \text{K}^+\text{I}^-} = 0.109$ and $\tau_{\text{K}^+\text{I}^-, \text{K}^+\text{Cl}^-} = 0.124$ [21], the solubility curves (Figure 3) were reproduced well. However, since the visibility of the respective curves in Figure 5 a) of [21] is restricted, no attempt was made to reproduce the fragments of the curve. Instead, only the experimental data compiled by Linke [60] are shown in Figure 3 for comparison.

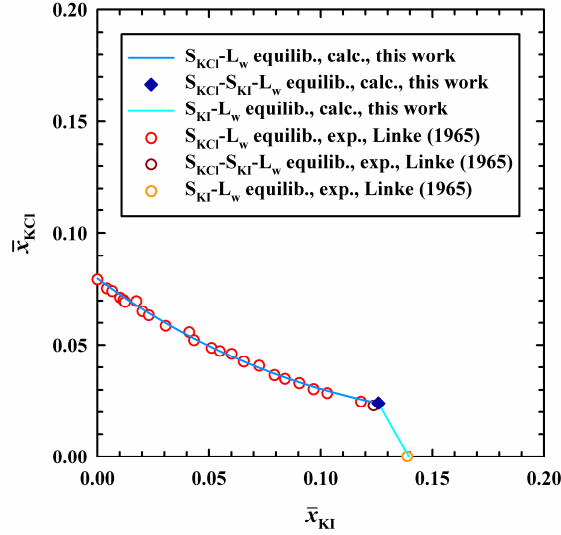


Figure 3 Salt Precipitation in the system $\{H_2O + KI + KCl\}$ at $T = 298.15$ K and ambient pressure. (—) $S_{KCl}L_w$ -, (\blacklozenge) $S_{KCl}S_{KI}L_w$ -, and (—) $S_{KI}L_w$ -equilibrium, this work. (O) experimental data [60] (data point at $S_{KCl}S_{KI}L_w$ equilibrium is the averaged value over the data points given in [60]).

3.2 Application of the eNRTL model to the description of gas hydrate equilibria

Four different aqueous ternary or quaternary electrolyte systems of the type $H_2O + CA + \text{gas}$ or $H_2O + C_1A + C_2A + \text{gas}$ have been modelled. The influence of the strong electrolytes NaCl, KCl and $CaCl_2$ on the HL_wG -phase equilibrium obtained in mixtures containing the hydrate forming gases methane (CH_4) and carbon dioxide (CO_2), respectively, was investigated. Values of the eNRTL solvent-salt parameters $B_{CA,w,0}$, $B_{CA,w,1}$ and $B_{CA,w,2}$ and $B_{w,CA,0}$, $B_{w,CA,1}$ and $B_{w,CA,2}$ for $CA = NaCl, KCl, CaCl_2$ were retrieved from the Aspen Properties[®] data bank of the Aspen Engineering Suite and are listed in Table 5. Salt-salt-parameters were set to zero. The influence of the amount of gas dissolved in the liquid phase on the activity coefficient of the solvent species $\gamma_{x,w}^{L_w}$ was neglected. With the eNRTL expression for $\gamma_{x,w}^{L_w}$ (eq. (8) in combination with eq. (17) and eq. (40) for $j \equiv w$), modelling calculations have been carried out on the three-phase $H-L_w-G$ -boundary p - T -lines of ternary and quaternary mixtures at different values of the ionic strengths involving gas hydrate phases.

Table 5 Ion-pair-water eNRTL parameters $B_{CA,w,0}$, $B_{CA,w,1}$ and $B_{CA,w,2}$, and water-ion-pair eNRTL parameters $B_{w,CA,0}$, $B_{w,CA,1}$ and $B_{w,CA,2}$ for $CA = NaCl, KCl, CaCl_2$ required for obtaining $\tau_{CA,w}(T)$ and $\tau_{w,CA}(T)$ according to eqs. (43) and (44).

Parameter ^a	NaCl	KCl	$CaCl_2$
$B_{CA,w,0}$	-3.789168	-4.060085	-5.06
$B_{CA,w,1}/K$	-216.3646	-30.93534	0.0
$B_{CA,w,2}$	-1.100418	1.42956	0.0
$B_{w,CA,0}$	5.980196	6.849537	10.472
$B_{w,CA,1}/K$	841.5181	402.9818	0.0

$B_{w,CA,2}$	7.4335	0.206522	0.0
--------------	--------	----------	-----

^a Retrieved from the data bank provided by Aspen Properties[®].

The Langmuir constant C_{ji} was expressed by means of eqs. (A.1)-(A.3) in terms of the microscopic quantities σ_{jw} , ε_{jw} , a_j , z_i and R_i . The Kihara parameters σ_{jw} and ε_{jw} were taken from our previous study [34], whereas the numerical values for the hard core radius a_j were taken from [35]. The complete set of Kihara parameters, including a comparison with values published in the literature for σ_{jw} and ε_{jw} [1,35], is compiled in Table 6. With regard to the radius R_i of the cavity of type i , $R_i = 395$ pm was used for the small 5^{12} - and $R_i = 433$ pm for the large $5^{12}6^2$ -cavity of sI hydrates, respectively, whereas $R_i = 391$ pm was used for the small 5^{12} - and $R_i = 473$ pm for the large $5^{12}6^4$ -cavity of sII hydrates, respectively [35]. For the coordination number z_i , the value 20 and 24 was employed for the small and large cavity of structure I, respectively, whereas the value of 20 and 28 was used for z_i of the small and the large cavity of structure II, respectively [35].

Table 6 Kihara parameters. σ_{jw} - and ε_{jw} -values obtained from a previous regression [34] along with corresponding literature data; a_j -values taken from [1,35]

	a_j/pm	σ_{jw}/pm	$\varepsilon_{jw}/(k_B\text{K})$
CH ₄	38.34 ^a	315.03 ^b	158.71 ^b
		314.393 ^c	155.593 ^c
		316.50 ^a	154.54 ^a
CO ₂	68.05 ^a	298.30 ^b	171.41 ^b
		297.638 ^c	175.405 ^c
		298.18 ^a	168.77 ^a

^a 2nd ed. of the monograph of Sloan [35].

^b Used in this study. Taken from our previous publication (data set of “Model 3”) [34].

^c 3rd ed. of the monograph of Sloan and Koh [1].

3.2.1 H-L_w-G-equilibrium in aqueous electrolyte systems containing methane

Modelling calculations on the incipient hydrate forming in the electrolyte systems {H₂O + NaCl + CH₄}, {H₂O + NaCl + KCl + CH₄} and {H₂O + NaCl + CaCl₂ + CH₄} were carried out for mixtures of given initial salt concentration in the liquid phase. The modelled results are presented in Figure 4 in terms of p - T -H-L_w-G -phase boundary lines along with corresponding experimental data of Dholabhai et al. (1991) [61].

For the systems {H₂O + NaCl + CH₄} and {H₂O + NaCl + KCl + CH₄} (Figure 4 a)), the model shows a good overall performance despite the relatively high pressure range ($2 < p/\text{MPa} < 10$) covered. The values for the Average Absolute Relative Deviation (AARD) between the experimental [61] and calculated pressures defined as

$$\left\langle \frac{|\Delta p|}{p} \right\rangle = \frac{1}{N_{\text{exp data}}} \sum_{q=1}^{N_{\text{exp data}}} \frac{|p_{\text{exp},q} - p_{\text{calc},q}|}{p_{\text{exp},q}} \quad (48)$$

range from 2.8 % for the mixture {H₂O + NaCl + CH₄} with $\bar{x}_{\text{NaCl}} = 0.0094$ to approximately 7.0 % for the two salt-system with $\bar{x}_{\text{NaCl}} = 0.0367$ and $\bar{x}_{\text{KCl}} = 0.0354$. The curves show the potential of the salts for acting as inhibitors with respect to the formation of gas hydrates since at $T = \text{const}$ the pressure rises with increasing salt concentration.

While for the system $\{\text{H}_2\text{O} + \text{NaCl} + \text{CaCl}_2 + \text{CH}_4\}$ (Figure 4 b)), the temperature and pressure range ($265 < T/\text{K} < 281$, $2 < p/\text{MPa} < 10$) as well as the AARD values relative to the data of Dholabhai et al. (1991) [61] are comparable with those of the previous mixtures (between 2 % and 6 %), the overall electrolyte concentration is smaller. However, since the 2-1-electrolyte CaCl_2 possesses a bivalent cation, the ionic strength range is not smaller. Not only does CaCl_2 release three ions in solution, but the Ca^{2+} -ion does also have a higher charge and charge density than the K^+ -ion, leading to an increased hydration of the Ca^{2+} -ion [62]. Nevertheless, the performance of the eNRTL model for this mixture is still very good.

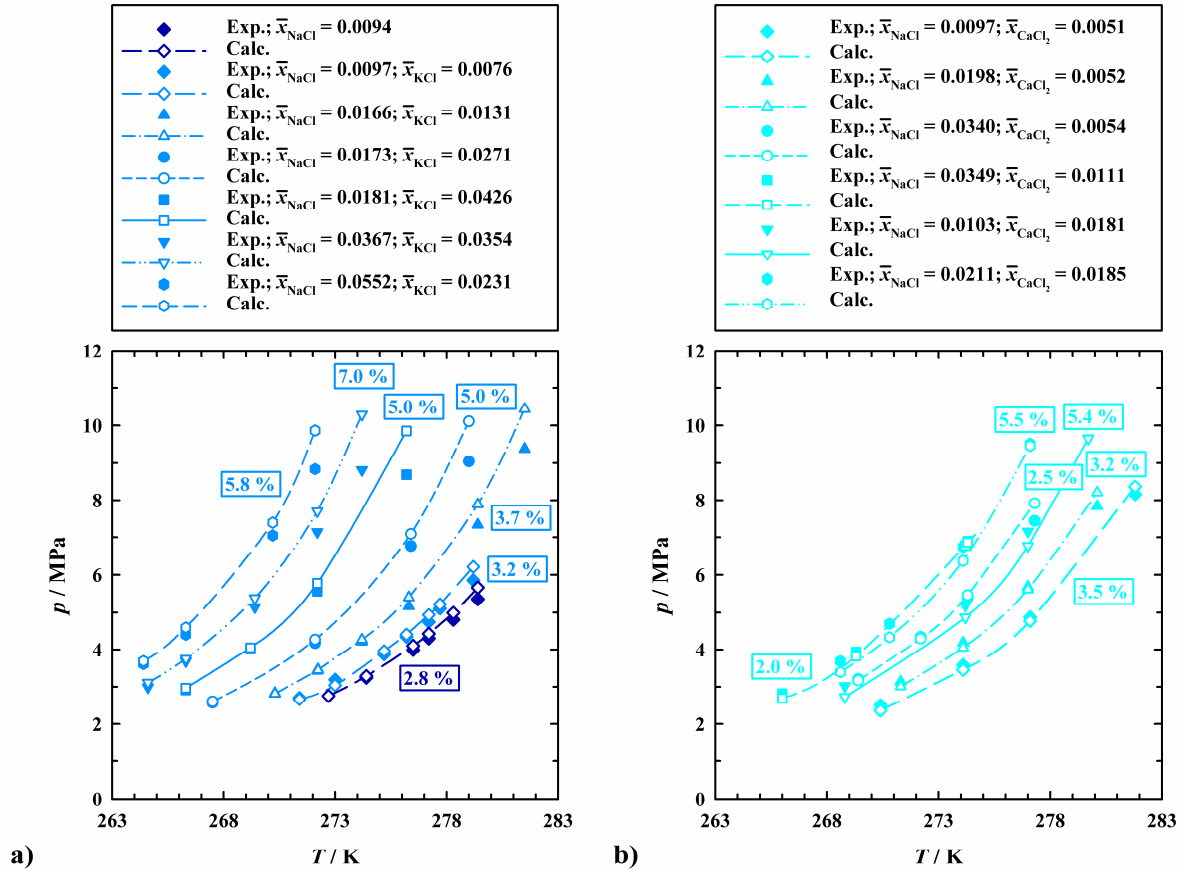


Figure 4 H-L_w-G- p - T equilibrium data in a) the systems $\{\text{H}_2\text{O} + \text{NaCl} + \text{CH}_4\}$ and $\{\text{H}_2\text{O} + \text{NaCl} + \text{KCl} + \text{CH}_4\}$ and in b) the system $\{\text{H}_2\text{O} + \text{NaCl} + \text{CaCl}_2 + \text{CH}_4\}$ at given overall mole fractions of the electrolytes. Lines and hollow symbols: modelling, solid symbols: experimental data of Dholabhai et al. (1991) [61].

3.2.2 H-L_w-G-equilibrium in aqueous electrolyte systems containing carbon dioxide

Incipient hydrate forming conditions have additionally been modelled for aqueous systems containing the same electrolytes as the ones treated in section 3.2.1, but with carbon dioxide instead of methane as the hydrate forming component (Figure 5).

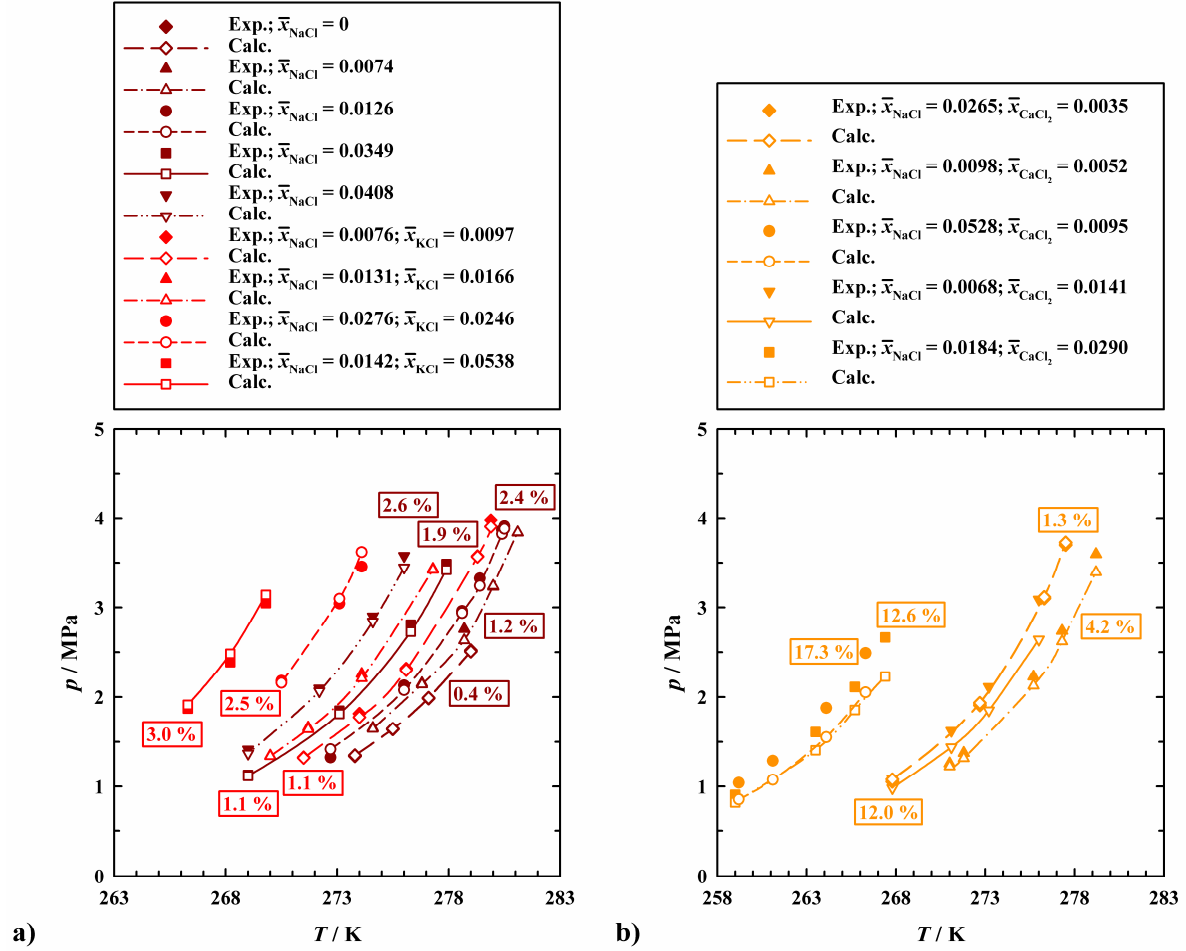


Figure 5 H-L_w-G-*p*-*T*-equilibrium in a) the systems {H₂O+CO₂}, {H₂O+NaCl+CO₂} and {H₂O+NaCl+KCl+CO₂}, respectively, and in b) the quaternary system {H₂O+NaCl+CaCl₂+CO₂} at given overall mole fractions of the electrolytes. Lines and hollow symbols: modelling, solid symbols: experimental data of Dholabhai et al. (1993) [63].

As can be seen in Figure 5 a), for the single salt system {H₂O+NaCl+CO₂} the maximum overall mole fraction of NaCl is $\bar{x}_{\text{NaCl}} = 0.04$, whereas for the system {H₂O+NaCl+KCl+CO₂} $\bar{x}_{\text{NaCl, max}} + \bar{x}_{\text{KCl, max}} \approx 0.07$. Within the pressure range of $0 < p/\text{MPa} < 4$ a very good performance of the eNRTL model is observed for this system with AARD values varying mostly between 1 and 2 %. Like in the mixtures with CH₄ (Figure 4), the curves in Figure 5 a) show that the strong electrolytes NaCl and KCl act as hydrate inhibitors, causing the temperature (at a given pressure) to fall, or the pressure (at a given temperature) to rise for hydrate formation with increasing salt mole fraction.

Our study is completed by the results of the modelling of the incipient hydrate forming conditions in the quaternary mixture {H₂O+NaCl+CaCl₂+CO₂}. The results (Figure 5 b)) reveal that on a similar pressure interval as in the previous example, higher deviations between calculated and experimental pressures are observed than for the other systems. Whereas the result for the two lowest concentrated mixtures is fairly good with AARD values with respect to the data of Dholabhai et al. (1993) [63] of 1.3 % and 4.2 % at $\bar{x}_{\text{NaCl}} = 0.0265$ and $\bar{x}_{\text{CaCl}_2} = 0.0035$, and $\bar{x}_{\text{NaCl}} = 0.0098$ and $\bar{x}_{\text{CaCl}_2} = 0.0052$, respectively, the deviations

increase up to values between 12 % and 18 % for the higher concentrated solutions. This is most probably due to the influence of the significantly higher degree of hydration of the Ca^{2+} -ion rather than due to neglecting the solubility of the CO_2 in the liquid phase in calculating $\gamma_{x,w}^{\text{L}_w}$. Moreover, since the salt-salt parameters between NaCl and CaCl_2 were not known, the interaction between the ions of the two salts had to be neglected as well.

4 Conclusion

In this article, it is demonstrated by numerous examples that the eNRTL-model of Chen and co-workers [15,20-23] has been implemented successfully in a Java programme. The eNRTL model implementation in turn was incorporated in a previously developed in-house programme enabling to perform, among other features, predictive calculations on H-L_w-G - phase boundaries of systems involving gas hydrates.

The correctness of the code has been verified by calculations on osmotic coefficients and mean ionic activity coefficients of binary solutions of strong electrolytes and ternary mixtures of the type {water + salt₁ + salt₂} where the constituting salts have one ion in common. The examples selected for this purpose were taken from the original articles on the eNRTL model by Chen and Evans [21] and Bollas et al. [23]. In case of the {H₂O + NaCl + LiCl} -mixture, the shape of the osmotic coefficient curves could not reproduced with the salt-salt-parameter values given in [21]. However, upon incrementing each of them by one, it turned out that the curves were reproduced at least qualitatively. Since the results of that calculation had also been checked independently by means of the computer algebra software “mathcad”, it is suspected that the sequence of the salt-salt coefficients given in [21] was reported erroneously. The data of the remaining systems could be reproduced from the original work. The results reveal once more, that the eNRTL model provides an accurate description of liquid phase non-ideality of the electrolyte systems over the ranges of state conditions investigated. The model does not only correlate thermodynamic data, but possesses also predictive capability using model parameters determined exclusively from data of the constituting binaries and ternary salt-salt systems with a common ion [21].

The model was subsequently used in the purely predictive modelling of H-L_w-G -hydrate phase equilibria of mixtures with water, one or two of the salts NaCl, KCl and CaCl_2 and methane or carbon dioxide using a set of Kihara parameters obtained in an earlier study [34]. In calculating $\gamma_{x,w}^{\text{L}_w}$, the presence of CO_2 in the liquid phase was neglected. Salt-salt-interaction parameters were also neglected. Despite of these simplifications, the p - T -values obtained reveal a good overall performance of the model leading to average absolute relative deviations ranging from 2 % to 7 %. Only at higher ionic strengths and when the bivalent Ca^{2+} -ion gets involved, the deviations increase remarkably to reach approximately 20 %. In a future work this deficiency may be overcome by implementing a model version that takes hydration into account [62]. Nevertheless, in view of the simplifications introduced, it can be stated that the results are quite satisfying from an engineering point of view.

Acknowledgement

This work has been carried out within the framework of the ANR (French Research Agency) project SECOHYA and the European iCap research project (EU FP7, GA No. 241393). We are grateful to Peter J. Herslund for inspiring discussions on several topics related to the thermodynamics of gas hydrates.

5 List of symbols

Normal symbols

a	a) Spherical hard core radius in Kihara potential $[a] = \text{pm}$; b) coefficients in Henry's constant correlation with temperature, dimensionless
A_ϕ	Debye-Hückel constant, dimensionless
A	Coefficient used in the temperature correlation for the eNRTL-parameters $\tau_{mm'}$ and $\tau_{m'm}$. $[A_1] = \text{K}$, $[A_3] = \text{K}^{-1}$, A_0 and A_2 , dimensionless
AARD	Average absolute relative deviation
α	Nonrandomness factor, dimensionless
b	Coefficient used in the correlation for $\Delta_\beta^{\text{Lw}} C_{p,m,w}^\circ(T, p_0)$ with temperature, $[b] = \text{J K}^{-2} \text{mol}^{-1}$
b_j	Molality of a chemical species j , $[b_j] = \text{mol kg}^{-1}$
\bar{b}_k	Overall or apparent molality of component k , $[\bar{b}_k] = \text{mol kg}^{-1}$
B	Coefficient used in temperature correlation of eNRTL-parameters $\tau_{CA,m}$, $\tau_{m,CA}$, $\tau_{AC,AC'}$, $\tau_{AC',AC}$, $\tau_{CA,CA'}$, $\tau_{CA',CA}$. $[B_1] = \text{K}$, B_0 and B_2 , dimensionless
c	Constant used for calculating the effective mole fractions X in eNRTL equations. c_j to be set to zero for $j \in S_m$, and to $ z_j $ for $j \in S_C \cup S_A$, respectively
C	a) Langmuir constant, $[C] = \text{Pa}^{-1}$; b) heat capacity, $[C] = \text{J K}^{-1}$
Δ	Finite difference between two values of a quantity
Δ_α^β	Finite difference between two values of a quantity for a process from initial state α to final state β
e	Elementary charge, $e = (1.602\,176\,565 \pm 0.000\,000\,035) \times 10^{-19} \text{ C}$ [41]
eNRTL	Electrolyte Non-Random-Two-Liquid model for the excess Gibbs energy
EOS	Equation of state
ε_{jw}	Characteristic energy between guest j and host water molecule w , $[\varepsilon] = \text{J}$
ε_0	Permittivity of free space, $[\varepsilon_0] = 8.854\,187\,817 \times 10^{12} \text{ F m}^{-1}$ [41]
ε_r	Relative permittivity, dimensionless
f	Fugacity, $[f] = \text{Pa}$
g	Molar interaction energy in the framework of the eNRTL model, $[g] = \text{J mol}^{-1}$
G	a) Gibbs energy, $[G] = \text{J}$; b) Boltzmann kind factor, dimensionless
γ	Activity coefficient, dimensionless
I	Ionic strength, dimensionless
k_B	Boltzmann constant, $k_B = (1.380\,648\,8 \pm 0.000\,001\,3) \times 10^{-23} \text{ J K}^{-1}$ [41]
$k_{H,j,w}$	Henry's constant of gas j in water, $[k_{H,j,w}] = \text{Pa}$
m	Mass, $[m] = \text{kg}$
M	Molar mass, $[M] = \text{g mol}^{-1}$
μ	Chemical potential of a species or component, $[\mu] = \text{J mol}^{-1}$

n	Amount of substance or mole number, $[n] = \text{mol}$
N	Number in general, dimensionless
NRTL	Non-Random-Two-Liquid model for the excess Gibbs energy
N_{Av}	Avogadro constant, $N_{\text{Av}} = (6.022\,141\,29 \pm 0.000\,000\,27) \times 10^{23} \text{ mol}^{-1}$ [41]
ν	a) Stoichiometric coefficient, dimensionless; b) number of water molecules per number of guest molecules in a cage of type i (hydration number), dimensionless
p	Pressure, $[p] = \text{Pa}$
R	Molar gas constant, $R = (8.314\,462\,1 \pm 0.000\,007\,5) \text{ J mol}^{-1} \text{ K}^{-1}$ [41]
ρ	a) Density, $[\rho] = \text{kg m}^{-3}$; b) Closest approach parameter, dimensionless
T	Absolute temperature, $[T] = \text{K}$
τ	Interaction energy eNRTL-parameter, dimensionless
θ_{ji}	Fraction of sites occupied by species j in cavity of type i , dimensionless
S	Given set (here of indices) in general
SAFT	Statistical Fluid Associated Solution Theory
σ_{jw}	Core distance at which attraction and repulsion between guest species j and host water molecule w in host-pair balance each other, $[\sigma_{jw}] = \text{pm}$
V	Volume, $[V] = \text{m}^3$
VRE	Variable Range for Electrolytes; particular model variant of the SAFT-EOS
\bar{w}_k	Overall or apparent weight fraction of component k , dimensionless
x_j	Mole fraction of chemical species j , dimensionless
\bar{x}_k	Overall or apparent mole fraction of component k , dimensionless
X_j	Effective mole fractions of species j , dimensionless
Y_j	Ionic charge fractions of ionic species $j = \text{C}, \text{A}$, dimensionless
z_j	Charge number of species j , positive for cations, negative for anions, zero for neutral species, dimensionless

Subscripts

$\text{A}, \text{A}', \text{A}''$	Anionic species $\text{A}^{ z_{\text{A}} -}$
b	Indicating reference to molality as composition
$\text{C}, \text{C}', \text{C}''$	Cationic species $\text{C}^{z_{\text{C}} +}$
CA	Binary salt $\text{C}_{\nu_{\text{C}}} \text{A}_{\nu_{\text{A}}}$, composed of ν_{C} cations, $\text{C}^{z_{\text{C}} +}$, and ν_{A} anions, $\text{A}^{ z_{\text{A}} -}$
cav	Referring to type of cavity
exp data	Referring to experimental data
fus	Property referring to the process of fusion
g	Referring to type of guest species
i	Type of cavity
j, l	Chemical species
k	Indicating components (molecular and strong electrolyte components)

LC	Local Composition model
LR	Property referring to Long Range contribution
m, m'	Referring to molecular species
m	Molar quantity
p	Referring to property at constant pressure
PDH	Referring to Pitzer-Debye-Hückel model
q	Index used for counting data points
SR	Property referring to Short Range contribution
w	Water (the only solvent component occurring in this study)
x	Indicating reference to mole fraction as composition variable
\pm	Mean ionic quantity
0	Reference conditions for temperature and pressure, $T_0 = 273.15 \text{ K}$, $p_0 = 0 \text{ MPa}$

Superscripts

–	Indicating a concentration quantity of component k based on the overall/apparent composition (possible dissociation or association reactions are thus disregarded)
*	Unsymmetric convention for the normalisation of the excess Gibbs energy and the activity coefficients
◦	Pure component state
∞	State of infinite dilution
β	Metastable empty hydrate phase
E	Excess property
G	Gas phase
H	Hydrate phase
I	Ice phase
L_w	Liquid aqueous phase
π	Any given phase in general
R	Residual Property
ref	Reference state/frame in general
S	Solid phase in general
σ	Liquid-vapour saturation conditions

A Appendix

A.1 The cell potential function and its relation to the Langmuir constant

The Langmuir constant C_{ji} reflects the intermolecular forces between the guest molecule j and the water molecules constituting the cavity of type i by which it is enclosed. Since these forces are in turn related to the host-guest interaction potential, C_{ji} can be calculated from a suitable expression for the potential energy ω_{ji} of species j in cavity i . In this study, the interaction potential energy was assumed to be describable by the cell potential $\omega_{ji}(r)$

presented by Parrish and Prausnitz [43] which assumes the cavities to be of spherically symmetrical geometry. In accordance with the suggestion of MacKoy and Sinanoğlu [45] this cell potential is based on the Kihara potential [64] as the underlying intermolecular pair potential energy model. In this model the effect of the finite size of the different interacting molecules is taken into account by ascribing a hard core to each molecule [45].

To arrive at the expression for $\omega_{ji}(r)$, the integral effect of the interactions between guest j and each of the nearest neighbouring host molecules within the type i cavity is obtained by means of the averaging procedure used in the cell theory of Lennard-Jones and Devonshire [65]. In applying the averaging method [65] to the assembly of the guest species and its nearest neighbouring spherically arranged water molecules, the guest molecule j is regarded as a spherical hard core of radius a_j [66], whereas the water molecules are approximated by point molecules. This leads to the following cell potential energy function [43]

$$\omega_{ji}(r) = 2z_i \varepsilon_{jw} \left(\frac{\sigma_{jw}^{12}}{R_i^{11} r} \left(\delta_{ji}(12) + \frac{a_j}{R_i} \delta_{ji}(11) \right) - \frac{\sigma_{jw}^6}{R_i^5 r} \left(\delta_{ji}(4) + \frac{a_j}{R_i} \delta_{ji}(5) \right) \right) \quad (\text{A.1})$$

where

$$\delta_{ji}(N) = \frac{1}{N} \left(\left(1 - \frac{r}{R_i} - \frac{a_j}{R_i} \right)^{-N} - \left(1 + \frac{r}{R_i} - \frac{a_j}{R_i} \right)^{-N} \right) \quad (\text{A.2})$$

In eq. (A.1) and (A.2), r is the distance between the centre of the cavity and the centre of the guest molecule, whereas σ_{jw} stands for the core distance at which attraction and repulsion balance each other. ε_{jw} denotes the characteristic maximum attractive potential energy. Along with a_j , σ_{jw} and ε_{jw} are referred to as the “Kihara parameters” which depend on the properties of guest species only. z_i and R_i are the coordination number and the radius of the spherically assumed cavity i . They have been uniquely determined for each cavity from x-ray diffraction experiments and are regarded as independent of the guest molecule [1].

It should be pointed out here that throughout the literature two different coordinate systems are used (as e.g. in [43,45,64,67]) for expressing the distance quantities and parameters appearing in the Kihara potential energy expression. Often, like in eqs. (A.1) and (A.2), different standards are even used in the same equation [68]: whereas σ_{jw} measures the shortest distance between the edge of the core and the water point molecule, r refers to the distance measured relative to the centre of the guest molecule. The various standards used for the distance quantities and the possible confusion arising from the inconsistent usage of these different standards have been reviewed by Bakker et al. (1996) [68] and Bakker (1998) [69].

The relation between the Langmuir constant C_{ji} and the potential energy $\omega_{ji}(r)$ of the guest molecule j in the spherically symmetrical cavity i is given by

$$C_{ji} = \frac{4\pi}{k_B T} \int_0^{R_i - a_j} \exp\left(-\frac{\omega_{ji}(r)}{k_B T}\right) r^2 dr \quad (\text{A.3})$$

where T denotes the thermodynamic temperature and k_B the Boltzmann constant [41], respectively. Although $\omega_{ji}(r)$ is not defined at $r = 0$, it can be shown that this discontinuity can be removed since the right-sided limes for $r \rightarrow 0+$ exists. Evaluation of the latter leads to

$$\lim_{r \rightarrow 0^+} \omega_{ji}(r) = 4z_i \varepsilon_j \left(\frac{\sigma_j}{R_i - a_j} \right)^6 \left(\left(\frac{\sigma_j}{R_i - a_j} \right)^6 - 1 \right) \quad (\text{A.4})$$

The lower limit of integration in the expression of eq. (A.3) can thus be set to zero. However, $\omega_{ji}(r)$ possesses another discontinuity at $r = R_i - a_j$ which in contrast to the former is a singularity with a change in sign that can not be removed. When approaching $R_i - a_j$ from the left side, $\omega_{ji}(r)$ tends to $+\infty$, when $R_i - a_j$ is approached from the right side, $\omega_{ji}(r)$ tends to $-\infty$. Therefore, since $\exp(-\omega_{ji}(r)/k_B T)$ diverges when $R_i - a_j$ is approached from the right side, the upper integration limit in eq. (A.3) has to be set to $R_i - a_j$. The region between $R_i - a_j$ and R_i is thus to be excluded from the integration interval.

A.2 The description of the chemical potential of water in the liquid phase

The difference between the chemical potential of water in the liquid and in the β -phase, $\Delta_{\beta}^{\text{L}_w} \mu_w(T, p, \bar{x}^{\text{L}_w})$, is calculated from the following classical thermodynamic relation

$$\frac{\Delta_{\beta}^{\text{L}_w} \mu_w(T, p, \bar{x}^{\text{L}_w})}{RT} = \frac{\Delta_{\beta}^{\text{L}_w} \mu_w^{\circ}(T_0, p_0)}{RT_0} - \int_{T_0}^T \frac{\Delta_{\beta}^{\text{L}_w} H_{\text{m},w}^{\circ}(T, p_0)}{RT^2} dT + \int_{p_0}^p \frac{\Delta_{\beta}^{\text{L}_w} V_{\text{m},w}^{\circ}(T, p)}{RT} dp + \ln a_w^{\text{L}_w}(T, p, \bar{x}^{\text{L}_w}) \quad (\text{A.5})$$

where \bar{x}^{L_w} and $a_w^{\text{L}_w} \equiv a_{x,w}^{\text{L}_w}$ denote the vector of independent mole fractions and the activity of water in the liquid phase, respectively. The activity of water is defined by means of its corresponding activity coefficient $\gamma_{x,w}^{\text{L}_w}$ as

$$a_w^{\text{L}_w} = x_w^{\text{L}_w} \gamma_{x,w}^{\text{L}_w}, \quad (\text{A.6})$$

$T_0 = 273.15 \text{ K}$ and $p_0 = 0 \text{ MPa}$ in eq. (A.5) are reference values for temperature and pressure [34]. $\Delta_{\beta}^{\text{L}_w} \mu_w^{\circ}(T_0, p_0)$ is the chemical potential difference at standard conditions. Assuming a linear empirical relationship for the molar isobaric heat capacity difference according to

$$\Delta_{\beta}^{\text{L}_w} C_{\text{m},w}^{\circ}(T, p_0) = \Delta_{\beta}^{\text{L}_w} C_{\text{m},w}^{\circ}(T_0, p_0) + b(T - T_0), \quad (\text{A.7})$$

and regarding the corresponding molar volume difference $\Delta_{\beta}^{\text{L}_w} V_{\text{m},w}^{\circ}(T, p)$ as constant by using its value at reference conditions, $\Delta_{\beta}^{\text{L}_w} V_{\text{m},w}^{\circ}(T_0, p_0)$, the integration of eq. (A.5) leads to eq. (4) when eqs. (A.6) and (A.7) are additionally taken into account. Thereby, use had to be made of the thermodynamic relationship $\Delta_{\beta}^{\text{L}_w} C_{\text{m},w}^{\circ}(T, p_0) = (\partial \Delta_{\beta}^{\text{L}_w} H_{\text{m},w}^{\circ}(T, p_0) / \partial T)_{p, \bar{x}}$.

A.3 On activity coefficients and the osmotic coefficient

The activity coefficient $\gamma_{x,j}$ describing the deviation of a given phase from an appropriately defined ideal mixture (mostly applied to quantify liquid phase non-idealities) can be derived from an expression for the excess molar Gibbs energy G_{m}^{E} according to

$$\ln \gamma_{x,j} = \frac{1}{RT} \left(\frac{\partial (n G_{\text{m}}^{\text{E}})}{\partial n_j} \right)_{T, p, n_{i \neq j}} \quad (\text{A.8})$$

where n is the total amount of substance on the basis of species and n_j is the amount of substance of species j . With the symmetrically referenced activity coefficient $\gamma_{x,j}$, the unsymmetrically referenced activity coefficient $\gamma_{x,j}^*$ can be derived by

$$\gamma_{x,j}^* = \frac{\gamma_{x,j}}{\gamma_{x,j}^\infty} \quad (\text{for all } j \in \{S_m \cup S_C \cup S_A\} \setminus \{w\}) \quad (\text{A.9})$$

where $\gamma_{x,j}^\infty$ stands for the activity coefficient at infinite dilution which is defined by

$$\gamma_{x,j}^\infty = \lim_{x_w \rightarrow 1} \gamma_{x,j} \quad (\text{A.10})$$

Care has to be taken when deriving activity coefficients of ions at infinite dilution in multi-component electrolyte systems in regard of whether or not this limiting value does exist in a strict mathematical sense (see remarks in appendix A.4).

The activity coefficient refers to the mole fraction (index x) as composition variable. Conversion to the value referring to molality (index b) is performed by

$$\gamma_{b,j}^* = \gamma_{x,j}^* x_w \quad (\text{for all } j \in \{S_m \cup S_C \cup S_A\} \setminus \{w\}) \quad (\text{A.11})$$

The mean ionic activity coefficient $\gamma_{x,CA,\pm}$ is, in contrast to the activity coefficient of the individual ions, an experimentally accessible quantity. It is defined in terms of the activity coefficients of the cation and the anion constituting the corresponding ion pair through

$$\ln \gamma_{x,CA,\pm} = \frac{\nu_{C,CA} \ln \gamma_{x,C} + \nu_{A,CA} \ln \gamma_{x,A}}{\nu_{C,CA} + \nu_{A,CA}} = \frac{z_C \ln \gamma_{x,A} + |z_A| \ln \gamma_{x,C}}{z_C + |z_A|} \quad (\text{A.12})$$

where $\nu_{C,CA}$ and $\nu_{A,CA}$ is the cationic and anionic stoichiometric coefficient of the cation-anion combination, respectively, and z_C and z_A is the charge number of the cation and the anion, respectively.

The (molal) osmotic coefficient ϕ is defined in terms of the activity coefficient of the solvent $\gamma_{x,w}$ as [9]

$$\phi = -\frac{\ln x_w + \ln \gamma_{x,w}}{M_w \sum_{j \in \{S_m \cup S_C \cup S_A\} \setminus \{w\}} b_j} \quad (\text{A.13})$$

where b_j designates the molality of species j .

A.4 The short range eNRTL-contribution to the activity coefficient for the ionic species

To derive the expressions for the activity coefficients of the ionic species, the calculation of the first partial derivative of the G_{SR}^E -function with respect to n_j , the mole number of species j , is required. Since the ionic charge fractions Y_C and Y_A appear in the expression for G_{SR}^E (explicitly and implicitly via the mixing rules for the concentration dependent model parameters), this step involves the calculation of $(\partial Y_C / \partial n_{j'})_{T,p,n_{l \neq j'}}$ and $(\partial Y_A / \partial n_{j'})_{T,p,n_{l \neq j'}}$. Calculating $(\partial Y_j / \partial n_{j'})_{T,p,n_{l \neq j'}}$ for $j = C$ (for all $C \in S_C$), implying $j'' = C''$ (for all $C'' \in S_C$), or $j = A$ (for all $A \in S_A$), implying $j'' = A''$ (for all $A'' \in S_A$), leads to

$$\left(\frac{\partial Y_j}{\partial n_{j'}} \right)_{T,p,n_{l \neq j'}} = \begin{cases} z_j Y_j (1 - Y_j) / (n X_j) & \text{for } j' = j \\ -z_{j''} Y_{j''} Y_j / (n X_{j''}) & \text{for } j' = j'' (\neq j), \\ 0 & \text{for } j' \neq j, j'' \end{cases} \quad (\text{A.14})$$

where it is understood that the indices j and j'' are taken from the same set of indices of ionic species, i.e., either cationic or anionic species, respectively, but that $j \neq j''$. $j' \neq j, j''$

means that j' originates from a set of a different type of species. In other words, the differentiation leads to the result that $(\partial Y_C / \partial n_{j'})_{T,p,n_{l \neq j'}}$ vanishes only for all $j' \in S_m \cup S_A$, but not for $j' \in S_C$ (the inverse holds for the derivative $(\partial Y_A / \partial n_{j'})_{T,p,n_{l \neq j'}}$, i.e., it vanishes for all $j' \in S_m \cup S_C$, but not for $j' \in S_A$). While the derivative vanishes in any case if it the differentiation is executed with respect to n_m ($m \in S_m$), it remains finite if the differentiation of Y_j is performed with respect to the mole number of an ion with a charge number of the same sign. Hence, taking the derivatives $(\partial Y_C / \partial n_{j'})_{T,p,n_{l \neq j'}}$ and $(\partial Y_A / \partial n_{j'})_{T,p,n_{l \neq j'}}$ correctly into account leads to expressions for $\ln \gamma_{x,C,SR}$ and $\ln \gamma_{x,A,SR}$ which are remarkably more complicated than the corresponding expression for $\ln \gamma_{x,m,SR}$. In the original publication on the multicomponent version of the eNRTL model, Chen and Evans [21] have set $(\partial Y_C / \partial n_{j'})_{T,p,n_{l \neq j'}} = (\partial Y_A / \partial n_{j'})_{T,p,n_{l \neq j'}} = 0$, apparently in order to simplify the calculations and resulting functions for $\ln \gamma_{x,C,SR}$ and $\ln \gamma_{x,A,SR}$. Only in 2008, Bollas et al. [23] presented an updated version of the model, in which the simplifying assumption of vanishing derivatives $(\partial Y_C / \partial n_{j'})_{T,p,n_{l \neq j'}}$ and $(\partial Y_A / \partial n_{j'})_{T,p,n_{l \neq j'}}$ made in deriving $\gamma_{x,C,SR}$ and $\gamma_{x,A,SR}$ had been removed. The quite lengthy most general expression for $\ln \gamma_{x,C,SR}$, derived within the framework of the model version of 2008, is given below. It was corrected for a typing error found in the original publication [23] and reads

$$\begin{aligned}
\frac{\ln \gamma_{x,C,SR}}{z_C} = & \sum_{A \in S_A} Y_A \frac{\sum_{j \in S_m \cup S_A} X_j G_{jC,AC} \tau_{jC,AC}}{\sum_{j' \in S_m \cup S_A} X_{j'} G_{j'C,AC}} \\
& + \sum_{m \in S_m} \frac{X_m}{\sum_{k \in S_m \cup S_C \cup S_A} X_k G_{km}} \left[G_{Cm} \left(\tau_{Cm} - \frac{\sum_{j \in S_m \cup S_C \cup S_A} X_j G_{jm} \tau_{jm}}{\sum_{j' \in S_m \cup S_C \cup S_A} X_{j'} G_{j'm}} \right) \right. \\
& + \sum_{A \in S_A} \frac{X_A}{\sum_{C' \in S_C} X_{C'}} \frac{(\alpha_{Am} G_{CA,m} - \alpha_{CA,m} G_{Am}) \tau_{Am} - (G_{CA,m} - G_{Am})}{\alpha_{Am}} \\
& \left. - \frac{\sum_{j \in S_m \cup S_C \cup S_A} X_j G_{jm} \tau_{jm}}{\sum_{j' \in S_m \cup S_C \cup S_A} X_{j'} G_{j'm}} \sum_{A \in S_A} \frac{X_A}{\sum_{C' \in S_C} X_{C'}} (G_{CA,m} - G_{Am}) \right] \\
& + \sum_{A \in S_A} X_A \left[\sum_{C' \in S_C} \frac{Y_{C'}}{\sum_{j' \in S_m \cup S_C} X_{j'} G_{j'A,C'A}} \left(G_{CA,C'A} \left(\tau_{CA,C'A} - \frac{\sum_{j \in S_m \cup S_C} X_j G_{jA,C'A} \tau_{jA,C'A}}{\sum_{j' \in S_m \cup S_C} X_{j'} G_{j'A,C'A}} \right) \right. \right. \\
& + \sum_{m \in S_m} \frac{X_m G_{mA,C'A}}{\sum_{C'' \in S_C} X_{C''}} \frac{(\alpha_{Am} G_{CA,m} - \alpha_{CA,m} G_{Am}) \tau_{mA,C'A} - (G_{CA,m} - G_{Am})}{\alpha_{Am} G_{Am}} \\
& \left. - \frac{\sum_{j \in S_m \cup S_C} X_j G_{jA,C'A} \tau_{jA,C'A}}{\sum_{j' \in S_m \cup S_C} X_{j'} G_{j'A,C'A}} \sum_{m \in S_m} \frac{X_m G_{mA,C'A}}{\sum_{C'' \in S_C} X_{C''}} \frac{G_{CA,m} - G_{Am}}{G_{Am}} \right) \\
& + \frac{1}{\sum_{C' \in S_C} X_{C'}} \left(\frac{\sum_{j \in S_m \cup S_C} X_j G_{jA,CA} \tau_{jA,CA}}{\sum_{j' \in S_m \cup S_C} X_{j'} G_{j'A,CA}} - \sum_{C' \in S_C} Y_{C'} \frac{\sum_{j \in S_m \cup S_C} X_j G_{jA,C'A} \tau_{jA,C'A}}{\sum_{j' \in S_m \cup S_C} X_{j'} G_{j'A,C'A}} \right) \quad (A.15)
\end{aligned}$$

Similarly, by applying eq. (A.8) to eq. (25) for $j=A$, the corresponding relation for $\ln \gamma_{x,A,SR}$ is derived [23].

$$\begin{aligned}
\frac{\ln \gamma_{x,A,SR}}{|z_A|} = & \sum_{C \in S_C} Y_C \frac{\sum_{j \in S_m \cup S_C} X_j G_{jA,CA} \tau_{jA,CA}}{\sum_{j' \in S_m \cup S_C} X_{j'} G_{j'A,CA}} \\
& + \sum_{m \in S_m} \frac{X_m}{\sum_{j' \in S_m \cup S_C \cup S_A} X_{j'} G_{j'm}} \left[G_{Am} \left(\tau_{Am} - \frac{\sum_{j \in S_m \cup S_C \cup S_A} X_j G_{jm} \tau_{jm}}{\sum_{j' \in S_m \cup S_C \cup S_A} X_{j'} G_{j'm}} \right) \right. \\
& + \sum_{C \in S_C} \frac{X_C}{\sum_{A' \in S_A} X_{A'}} \frac{(\alpha_{Cm} G_{CA,m} - \alpha_{CA,m} G_{Cm}) \tau_{Cm} - (G_{CA,m} - G_{Cm})}{\alpha_{Cm}} \\
& - \frac{\sum_{j \in S_m \cup S_C \cup S_A} X_j G_{jm} \tau_{jm}}{\sum_{j' \in S_m \cup S_C \cup S_A} X_{j'} G_{j'm}} \sum_{C \in S_C} \frac{X_C}{\sum_{A' \in S_A'} X_{A'}} (G_{CA,m} - G_{Cm}) \Big] \\
& + \sum_{C \in S_C} X_C \left[\sum_{A' \in S_A} \frac{Y_{A'}}{\sum_{j' \in S_m \cup S_C} X_{j'} G_{j'C,A'C}} \left(G_{AC,A'C} \left(\tau_{AC,A'C} - \frac{\sum_{j \in S_m \cup S_A} X_j G_{jC,A'C} \tau_{jC,A'C}}{\sum_{j' \in S_m \cup S_A} X_{j'} G_{j'C,A'C}} \right) \right. \right. \\
& + \sum_{m \in S_m} \frac{X_m G_{mC,A'C}}{\sum_{A'' \in S_A} X_{A''}} \frac{(\alpha_{Cm} G_{CA,m} - \alpha_{CA,m} G_{Cm}) \tau_{mC,A'C} - (G_{CA,m} - G_{Cm})}{\alpha_{Cm} G_{Cm}} \\
& - \frac{\sum_{j \in S_m \cup S_A} X_j G_{jC,A'C} \tau_{jC,A'C}}{\sum_{j' \in S_m \cup S_A} X_{j'} G_{j'C,A'C}} \sum_{m \in S_m} \frac{X_m G_{mC,A'C}}{\sum_{A'' \in S_A} X_{A''}} \frac{G_{CA,m} - G_{Cm}}{G_{Cm}} \Big) \\
& + \frac{1}{\sum_{A'' \in S_A} X_{A''}} \left(\frac{\sum_{j \in S_m \cup S_A} X_j G_{jC,AC} \tau_{jC,AC}}{\sum_{j' \in S_m \cup S_A} X_{j'} G_{j'C,AC}} - \sum_{A' \in S_A} Y_{A'} \frac{\sum_{j \in S_m \cup S_A} X_j G_{jC,A'C} \tau_{jC,A'C}}{\sum_{j' \in S_m \cup S_A} X_{j'} G_{j'C,A'C}} \right) \Big] \quad (A.16)
\end{aligned}$$

From eqs. (A.15) and (A.16), the corresponding activity coefficients at infinite dilution, $\gamma_{x,C,SR}^\infty$ and $\gamma_{x,A,SR}^\infty$, can be derived by applying eq. (A.10). The latter in turn enable the calculation of the unsymmetrically referenced activity coefficients $\gamma_{x,C,SR}^*$ and $\gamma_{x,A,SR}^*$ using eq. (A.9). Upon deriving $\ln \gamma_{x,C,SR}^\infty$ and $\ln \gamma_{x,A,SR}^\infty$ it was found that the corresponding expressions given in the original article of Bollas et al. [23] for the most general case of different nonrandomness parameters are erroneous. Moreover, an additional remark not made in [23] should be made here with regard to the calculation of the limiting value according to eq. (A.10). In fact, for the case of multielectrolyte solutions, i.e. if the number of different ionic species exceeds 2, the limiting value for $x_w \rightarrow 1$ of at least some of the quantities depending on the ionic charge fractions Y_j can not be calculated in the strict mathematical sense. More precisely, the limiting value for identically vanishing mole fractions of all species other than the solvent species is diverging and hence can not be calculated for all those Y_j depending quantities whenever $Y_j \neq 1$. $Y_j \neq 1$ in turn is necessarily observed when more than

one ion occurs in the respective expression for Y_C or Y_A . However, if it is assumed that the relative composition of all solute species remains constant during the limiting process of approaching the state of infinite dilution, the respective quantities causing problems could be evaluated. In order to indicate that these quantities refer to limiting values obtained in this “approximate way”, they are endowed with the superscript “ ∞ ” as well. The complication outlined above does not appear for a solution containing besides the solvent and any number of molecular solutes only one single electrolyte, that generates only two ions when being dissolved, since Y_j is unity for both $j = C$ and $j = A$, respectively.

A further remark should be added in this context. The fact that the limiting value of Y_j for $x_w \rightarrow 1$, and thus $\gamma_{x,C,SR}^\infty$ and/or $\gamma_{x,A,SR}^\infty$, may not exist does not have the consequence that the corresponding limiting values of $\gamma_{x,C,SR}^*$ and $\gamma_{x,A,SR}^*$ do not exist either. Due to a compensation of terms after normalisation of the expressions for $\gamma_{x,C,SR}$ and $\gamma_{x,A,SR}$, the limiting values $\gamma_{x,C,SR}^{*,\infty}$ and $\gamma_{x,A,SR}^{*,\infty}$ do exist. In particular, as expected and in accordance with the Henry’s law reference frame $\gamma_{x,C,SR}^{*,\infty} = \gamma_{x,A,SR}^{*,\infty} = 1$ for all $C \in S_C$ and $A \in S_A$.

With the conventions outlined above, the expression for $\ln \gamma_{x,C,SR}^\infty$, corrected for the error found in [23], reads

$$\begin{aligned} \frac{\ln \gamma_{x,C,SR}^\infty}{z_C} = & \frac{1}{z_C} \lim_{x_w \rightarrow 1} (\ln \gamma_{x,C,SR}) = \sum_{A \in S_A} Y_A^\infty \tau_{wC,AC}^\infty + G_{Cw}^\infty \tau_{Cw}^\infty \\ & + \sum_{A \in S_A} \frac{X_A^\infty}{\sum_{C' \in S_C} X_{C'}^\infty} \frac{(\alpha_{Aw}^\infty G_{CA,w} - \alpha_{CA,w} G_{Aw}^\infty) \tau_{Aw}^\infty - (G_{CA,w} - G_{Aw}^\infty)}{\alpha_{Aw}^\infty} , \quad (A.17) \\ & + \sum_{A \in S_A} X_A^\infty \left(\frac{\sum_{C' \in S_C} \frac{Y_{C'}^\infty}{\sum_{C'' \in S_C} X_{C''}^\infty} \left(\frac{(\alpha_{Aw}^\infty - \alpha_{CA,w}) G_{Aw}^\infty \tau_{wA,C'A}^\infty - (G_{CA,w} - G_{Aw}^\infty)}{\alpha_{Aw}^\infty G_{Aw}^\infty} \right)}{+ \frac{1}{\sum_{C'' \in S_C} X_{C''}^\infty} \left(\tau_{wA,CA}^\infty - \sum_{C' \in S_C} Y_{C'}^\infty \tau_{wA,C'A}^\infty \right)} \right) \end{aligned}$$

whereas the correct expression for $\ln \gamma_{x,A,SR}^\infty$ reads

$$\begin{aligned} \frac{\ln \gamma_{x,A,SR}^\infty}{|z_A|} = & \frac{1}{|z_A|} \lim_{x_w \rightarrow 1} (\ln \gamma_{x,A,SR}) = \sum_{C \in S_C} Y_C^\infty \tau_{wA,CA}^\infty + G_{Aw}^\infty \tau_{Aw}^\infty \\ & + \sum_{C \in S_C} \frac{X_C^\infty}{\sum_{A' \in S_A} X_{A'}^\infty} \frac{(\alpha_{Cw}^\infty G_{CA,w} - \alpha_{CA,w} G_{Cw}^\infty) \tau_{Cw}^\infty - (G_{CA,w} - G_{Cw}^\infty)}{\alpha_{Cw}^\infty} \quad (A.18) \\ & + \sum_{C \in S_C} X_C^\infty \left(\frac{\sum_{A' \in S_A} \frac{Y_{A'}^\infty}{\sum_{A'' \in S_A} X_{A''}^\infty} \left(\frac{(\alpha_{Cw}^\infty - \alpha_{CA,w}) G_{Cw}^\infty \tau_{wA,C'A}^\infty - (G_{CA,w} - G_{Cw}^\infty)}{\alpha_{Cw}^\infty G_{Cw}^\infty} \right)}{+ \frac{1}{\sum_{A'' \in S_A} X_{A''}^\infty} \left(\tau_{wC,AC}^\infty - \sum_{A' \in S_A} Y_{A'}^\infty \tau_{wC,A'C}^\infty \right)} \right) \end{aligned}$$

A.5 On the number of (isothermal) eNRTL parameters

The following coefficients are to be considered by the model: For a set $S_m = \{m_1, \dots, m_{N_m}\}$ of $N_m = |S_m|$ different molecular components, a set $S_C = \{C_1, \dots, C_{N_C}\}$ of $N_C = |S_C|$ different cations and a set $S_A = \{A_1, \dots, A_{N_A}\}$ of $N_A = |S_A|$ different anions, the following types of isothermal eNRTL coefficients have to be considered and the corresponding numerical values to be provided: a) $\alpha_{mm'}, \tau_{mm'}, \tau_{m'm}$, with $m < m'$ for all $m, m' \in S_m$, b) $\alpha_{m,CA}, \tau_{m,CA}, \tau_{CA,m}$, for all $m \in S_m, C \in S_C$ and $A \in S_A$, c) $\alpha_{CA,C'A}, \tau_{CA,C'A}, \tau_{C'A,CA}$, for all $C, C' \in S_C$ with $C < C'$ and $A \in S_A$ and d) $\alpha_{AC,A'C}, \tau_{AC,A'C}, \tau_{A'C,AC}$ for all $A, A' \in S_A$ with $A < A'$ and $C \in S_C$. Combinatorial considerations lead to the total number of isothermal coefficients N_{coeff} necessary to describe the multicomponent electrolyte system

$$\begin{aligned} N_{\text{coeff}} &= \left| \left\{ \alpha_{mm'}, \tau_{mm'}, \tau_{m'm} \right\} \right| + \left| \left\{ \alpha_{m,CA}, \tau_{m,CA}, \tau_{CA,m} \right\} \right| + \left| \left\{ \alpha_{CA,C'A}, \tau_{CA,C'A}, \tau_{C'A,CA} \right\} \right| \\ &\quad + \left| \left\{ \alpha_{AC,A'C}, \tau_{AC,A'C}, \tau_{A'C,AC} \right\} \right| \\ &= \frac{3}{2} \left(N_m (N_m - 1) + N_C N_A (2N_m + N_C + N_A - 2) \right) \end{aligned} \quad (\text{A.19})$$

If it is assumed in accordance with a very common approximation in the eNRTL-model that for the salt-salt interaction parameters the following relation is obeyed

$$\tau_{CA,C'A} = -\tau_{C'A,CA} \quad (\text{A.20})$$

$$\tau_{AC,A'C} = -\tau_{A'C,AC} \quad (\text{A.21})$$

and that for the non-randomness factors $\alpha_{mm'}$ (for the case of $N_m > 1$)

$$\forall_{m \in S_m} \forall_{\substack{m' \in S_m \\ m' > m}} \left(\alpha_{mm'} = \alpha_0 \right) \quad (\text{A.22})$$

and the non-randomness factors $\alpha_{m,CA}, \alpha_{CA,C'A}$ and $\alpha_{AC,A'C}$ the relations $\alpha_{m,CA} = \alpha_1$ (for all $m \in S_m, C \in S_C$ and $A \in S_A$), $\alpha_{CA,C'A} = \alpha_1$ (for all $C, C' \in S_C$ with $C < C'$ and $A \in S_A$) and $\alpha_{AC,A'C} = \alpha_1$ (for all $A, A' \in S_A$ with $A < A'$ and $C \in S_C$) do hold, the number of isothermal parameters N_{coeff} required to describe the system is given by

$$N_{\text{coeff}} = N_m (N_m - 1) + N_C N_A \left(2N_m + \frac{1}{2} N_C + \frac{1}{2} N_A - 1 \right) + 2 - \delta_{1N_m}, \quad (\text{A.23})$$

where δ_{1N_m} is Dirac's delta function, defined by

$$\delta_{1N_m} = \begin{cases} 0 & \text{for } N_m \neq 1 \\ 1 & \text{for } N_m = 1 \end{cases} \quad (\text{A.24})$$

If it is, however, assumed that $\tau_{CA,C'A} = \tau_{C'A,CA} = \tau_{AC,A'C} = \tau_{A'C,AC} = 0$ and $\alpha_{mm'} = \alpha_0$ (for all $m \in S_m$ and $m' \in S_m$ with $m' > m$) does hold along with $\alpha_{m,CA} = \alpha_1$ (for all $m \in S_m, C \in S_C$ and $A \in S_A$) and the assumption that $\alpha_{CA,C'A}$ (for all $C, C' \in S_C$ with $C < C'$ and $A \in S_A$) and $\alpha_{AC,A'C}$ (for all $A, A' \in S_A$ with $A < A'$ and $C \in S_C$) take any but finite values (since they are not needed), the number of isothermal parameters N_{coeff} needed to characterise the system is to be calculated from

$$N_{\text{coeff}} = N_m (N_m + 2N_C N_A - 1) + 2 - \delta_{1N_m} \quad (\text{A.25})$$

References

- [1] Sloan, E. D.; Koh, C. A.; "Clathrate Hydrates of Natural Gases"; CRC Press, Taylor & Francis Group, Boca Raton, London, New York, 3rd ed. (2008).
- [2] Ribeiro Jr., C. P.; Lage, P. L. C.; "Modelling of hydrate formation kinetics: State-of-the-art and future directions"; Chem. Eng. Sci. 63 (2008) 2007-2034.
- [3] Englezos, P.; "Clathrate Hydrates"; Ind. Eng. Chem. Res. 32 (1993) 1251-1274.
- [4] Sloan, E. D.; "Fundamental principles and applications of natural gas hydrates"; Nature 46 (2003) 353-359.
- [5] Eslamimanesh, A.; Mohammadi, A. H.; Richon, D.; Naidoo, P. Ramjugernath, D.; "Application of gas hydrate formation in separation processes: A review of experimental studies"; J. Chem. Thermodynamics 46 (2012) 62-71.
- [6] Barker, J. W.; Gomez, R. K.; "Formation of hydrates during deepwater drilling operations"; J. Petrol. Technol. 41 (1989) 297-301.
- [7] Hsieh, M.-K.; Yeh, Y.-T.; Chen, Y.-P.; Chen, P.-C.; Lin, S.-T.; Chen, L.-J.; "Predictive Method for the Change in Equilibrium Conditions of Gas Hydrates with Addition of Inhibitors and Electrolytes"; Ind. Eng. Chem. Res. 51 (2012) 2456-2469.
- [8] Clarke, M. A.; Bishnoi, P. R.; "Development of a new equation of state for mixed salt and mixed solvent systems, and application to vapour-liquid and solid (hydrate)-vapour-liquid equilibrium calculations"; Fluid Phase Equilib. 220 (2004) 21-35.
- [9] Luckas, M.; Krissmann, J.; "Thermodynamik der Elektrolytlösungen – Eine einheitliche Darstellung der Berechnung komplexer Gleichgewichte"; Springer-Verlag, Berlin, Heidelberg, New York (2001).
- [10] Fürst, W.; Renon, H.; "Representation of excess properties of electrolyte solutions using a new equation of state"; AIChE J. 39 (1993) 335-343.
- [11] Zuo, J. Y.; Zhang, D.; Fürst, W.; "Extension of the electrolyte EOS of Fürst and Renon to mixed solvent electrolyte systems"; Fluid Phase Equilib. 175 (2000) 285-310.
- [12] Trebble, M. A.; Bishnoi, P. R.; "Development of a new four-parameter cubic equation of state"; Fluid Phase Equilib. 35 (1987) 1-18.
- [13] Trebble, M. A.; Bishnoi, P. R.; "Extension of the Trebble-Bishnoi equation of state to fluid mixtures"; Fluid-Phase Equilib. 40 (1988) 1-21.
- [14] Galindo, A.; Gil-Villegas, A.; Jackson, G.; Burgess, A. N.; "SAFT-VRE: Phase Behavior of Electrolyte Solutions with the Statistical Associating Fluid Theory for Potentials of Variable Range"; J. Phys. Chem. B 103 (1999) 10272-10281.
- [15] Chen, C.-C.; Song, Y.; "Generalized Electrolyte-NRTL Model for Mixed-Solvent Electrolyte Systems"; AIChE J. 50 (2004) 1928-1941.
- [16] Bromley, L. A.; "Thermodynamic Properties of Strong Electrolytes in Aqueous Solution"; AIChE J. 19 (1973) 313-320.

- [17] Pitzer, K. S.; "Thermodynamics of Electrolytes. I. Theoretical Basis and General Equations"; J. Phys. Chem. 77 (1973) 268-277.
- [18] Pitzer, K. S.; "Electrolytes: From Dilute Solutions to Fused Salts"; J. Am. Chem. Soc. 102 (1980) 2902-2906.
- [19] Cruz, J. L.; Renon, H.; "A New Thermodynamic Representation of Binary Electrolyte Solutions Nonideality in the Whole Range of Concentrations"; AIChE J. 24 (1978) 817-830.
- [20] Chen, C.-C.; Britt, H. I.; Boston, J. F.; Evans, L.B.; "Local Composition Model for Excess Gibbs Energy of Electrolyte Systems"; AIChE J. 28 (1982) 588-596.
- [21] Chen, C.-C., Evans, L. B.; "A Local Composition Model for the Excess Gibbs Energy of Aqueous Electrolyte Systems"; AIChE J. 32 (1986) 444-454.
- [22] Chen, C.-C.; Bokis, C. P.; Mathias, P. M.; "A Segment-Based Excess Gibbs Energy Model for Aqueous Organic Electrolyte Systems"; AIChE J., 47 (2001) 2593-2602.
- [23] Bollas, G. M., Chen, C. C., Barton, P. I.; "Refined Electrolyte-NRTL Model: Activity Coefficient Expressions for Application to Multi-Electrolyte Systems"; AIChE J. 54 (2008) 1608-1624.
- [24] Li, J; Polka, H. M.; Gmehling, J.; "A g^E model for single and mixed solvent electrolyte systems 1. Model and results for strong electrolytes." Fluid Phase Equilibria, 94 (1998) 89-114
- [25] Papaiconomou, N.; Simonin, J.-P.; Bernard, O.; Kunz, W.; "MSA-NRTL Model for the Description of the Thermodynamic Properties of Electrolyte Solutions"; Phys. Chem. Chem. Phys. 4 (2002) 4435-4443.
- [26] van der Waals, J. H.; Platteeuw, J. C.; "Clathrate solutions"; Adv. Chem. Phys. 2 (1959) 1-57.
- [27] Englezos, P.; Bishnoi, P. R. Bishnoi; "Prediction of Gas Hydrate Formation Conditions in Aqueous Electrolyte Solutions"; AIChE J. 34 (1988) 1718-1721.
- [28] Meissner, H. P.; Kusik, C. L.; "Activity Coefficients of Strong Electrolytes in Multicomponent Aqueous Electrolyte Solutions"; AIChE J. 18 (1972) 294-.
- [29] Stryjek, R.; Vera, J. H.; "PRSV: An Improved Peng-Robinson Equation of State for Pure Compounds and Mixtures"; Can. J. Chem. Eng. 64 (1986) 323-333.
- [30] Michelsen, M. L.; "A Modified Huron-Vidal Mixing Rule for Cubic Equations of State"; Fluid Phase Equilib. 60 (1990) 213-219.
- [31] Yan, W. D.; Topphoff, M.; Rose, C.; Gmehling, J.; "Prediction of Vapour-Liquid Equilibria in Mixed-Solvent Electrolyte Systems Using the Group Contribution Concept"; Fluid Phase Equilib. 227 (2005) 157-164.
- [32] Hsieh, C. M.; Sandler, S. I.; Lin, S. T.; "Improvements of COSMO-SAC for Vapour-Liquid and Liquid-Liquid Equilibrium Predictions"; Fluid Phase Equilib. 297 (2010) 90-97.

- [33] Hsieh, M. T.; Lin, S. T.; “A Predictive Model for the Excess Gibbs Free Energy of Fully Dissociated Electrolyte Solutions”; *AIChE J.* 57 (2011) 1061-1074.
- [34] Herri J.-M.; Bouchemoua, A.; Kwaterski, M.; Fezoua, A.; Ouabbas, Y.; Cameirao, A.; “Gas Hydrate Equilibria for CO₂-N₂ and CO₂-CH₄ gas mixtures – Experimental studies and Thermodynamic Modelling”, *Fluid Phase Equilib.* 301 (2011) 171-190.
- [35] Sloan, E.D.; “Clathrate hydrates of natural gases”; 2nd ed., Marcel Dekker, New York, Basel (1997).
- [36] Matthias Kwaterski; Jean-Michel Herri; “Thermodynamic Modelling of Gas Semi-Clathrate Hydrates using the electrolyte NRTL Model”, under preparation
- [37] Belvèze, L. S., Brennecke, J. F., Stadtherr, M. A.; „Modeling of Activity Coefficients of Aqueous Solutions of Quaternary Ammonium Salts with the Electrolyte-NRTL Equation”; *Ind. Eng. Chem. Res.* 43 (2004) 815-825.
- [38] Lindenbaum, S.; Boyd, G. E.; “Osmotic and Activity Coefficients for the Symmetrical Tetraalkyl Ammonium Halides in Aqueous Solution at 25 °C”. *J. Phys. Chem.* 68 (1964) 911-917.
- [39] Ballard, A. L.; Sloan Jr., E. D.; “The next generation of hydrate prediction I. Hydrate standard states and incorporation of spectroscopy”; *Fluid Phase Equilib.* 194-197 (2002) 371-383.
- [40] “A Report of IUPAC Commission 1.2 on Thermodynamics Notation for states and processes, significance of the word ‘standard’ in chemical thermodynamics, and remarks on commonly tabulated forms of thermodynamic functions”; *J. Chem. Thermodyn.* 14 (1982) 805-815.
- [41] Mohr, P. J.; Taylor, B. N.; Newell, D. B.; “CODATA Recommended Values of the Fundamental Physical Constants: 2010”; *J. Phys. Chem. Ref. Data*, 41 (2012) 1-84.
- [42] Soave, G.; “Equilibrium constants from a modified Redlich-Kwong equation of state”; *Chem. Eng. Sci.* 27 (1972) 1197-1203.
- [43] Parrish, W.R.; Prausnitz, J.M.; “Dissociation pressure of gas hydrates formed by gas mixtures”; *Ind. Eng. Chem. Process Des. Develop.* 11 (1972) 26-35.
- [44] Kihara, T.; “The second virial coefficient of non-spherical molecules”; *J. Phys. Soc. Japan* 6 (1951) 289–296.
- [45] McKoy, V.; Sinanoğlu, O. J.; “Theory of dissociation pressures of some gas hydrates”; *J Chem. Phys* 38 (1963) 2946-2956.
- [46] Holder, G. D.; Corbin, G.; Papadopoulos, K. D.; “Thermodynamic and Molecular Properties of Gas Hydrates from Mixtures Containing Methane, Argon and Krypton”; *Ind. Eng. Chem. Fundam.* 19 (1980) 282-286.
- [47] Dharmawandhana, P. B.; “The measurement of the thermodynamic parameters of the hydrate structure and application of them in the prediction of natural gas hydrates”, PhD Thesis, Colorado School of Mines, Golden, CO, USA (1980).

- [48] John, V. T.; Papadopoulos, K. D.; Holder, G. D.; "A Generalized Model for Predicting Equilibrium Conditions for Gas Hydrates"; *AIChE J.* 31 (1985) 252-259.
- [49] Handa, Y. P.; Tse, J. S.; "Thermodynamic properties of empty lattices of structure I and structure II clathrate hydrates"; *J. Phys. Chem.* 90 (1986) 5917-5921.
- [50] Von Stackelberg, M.; Müller, H. R.; "On the structure of gas hydrates"; *J. Chem. Phys.* 19 (1951) 1319-1320.
- [51] Holder, G.D.; Zetts, S.P.; Pradhan, N.; "Phase behavior in systems containing clathrate hydrates, a review"; *Rev. Chem. Eng.* 5 (1988) 1-70.
- [52] McMillan W. G., Mayer J. E.; "The statistical thermodynamics of multicomponent systems"; *J. Chem. Phys.* 13 (1945) 276-305.
- [53] Aspen Technology, Inc.; "Aspen Physical Property System-Physical Property Models"-Manual; Vers. Nr. V7.1; 01/2009; 200 Wheeler Road Burlington, MA, USA.
- [54] Renon, H.; Prausnitz, J. M.; "Local Compositions in Thermodynamic Excess Functions for Liquid Mixtures"; *AIChE J.* 14 (1968) 135-144.
- [55] Austgen, D. M.; Rochelle, G. T.; Peng, X.; Chen, C.-C.; "Model of Vapor-Liquid Equilibria for Aqueous Acid Gas-Alkanolamine Systems Using the Electrolyte-NRTL Equation"; *Ind. Eng. Chem. Res.* 28 (1989) 1060-1073.
- [56] Danesh, A.; "PVT and Phase Behaviour of Petroleum Reservoir Fluids"; Elsevier (1998).
- [57] Mock B.; Evans, L. B.; Chen, C. C.; "Thermodynamic representation of phase-equilibria of mixed-solvent electrolyte systems"; *AIChE. J.* 32 (1986) 1655-1664.
- [58] Robinson, R. A.; Stokes, R. H.; "Electrolyte Solutions, 2nd rev. ed., Dover publications; Inc., Mineola, New York (2002). Reprint of the rev. ed. 1970.
- [59] Downloaded from "<http://www.southalabama.edu/physics/software/plotdigitizer.htm>", Department of Physics, University of South Alabama, Mobile, AL 36688, USA
- [60] Linke, W. F.; "Solubilities. Inorganic and Metal-Organic Compounds"; 4th ed., Am. Chem. Soc. Washington, DC, II (1965).
- [61] Dholabhai, P.D.; Englezos, P.; Kalogerakis, N.; Bishnoi, P.R.; "Equilibrium conditions for methane hydrate formation in aqueous mixed electrolyte solutions"; *Can. J. Chem. Eng.* 69 (1991) 800-805.
- [62] Chen C.-C.; Mathias, P. M.; and Orbey, H.; "Use of hydration and dissociation chemistries with the electrolyte-NRTL model"; *AIChE J.* 45 (1999) 1576-1586.
- [63] Dholabhai, P.D.; Kalogerakis, N.; Bishnoi, P.R.; "Equilibrium conditions for carbon dioxide hydrate formation in aqueous electrolyte solutions". *J. Chem. Eng. Data* 38 (1993) 650-654.
- [64] Kihara, T.; "The second virial coefficient of non-spherical molecules"; *J. Phys. Soc. Japan* 6 (1951) 289-296.

- [65] Lennard-Jones, J.E.; Devonshire, A. F.; “Critical Phenomena in Gases. I”; Proc. R. Soc. Lond. A 163 (1937) 53-70.
- [66] Mooijer-van den Heuvel, M. M.; “Phase Behaviour and Structural Aspects of Ternary Clathrate Hydrate Systems”; PhD thesis, Technical University of Delft, The Netherlands (2004).
- [67] Tee, L. S.; Gotoh, S.; Stewart, W. E.; “Molecular Parameters for Normal Fluids – The Kihara Potential with a spherical core”; Ind. Eng. Chem. Fundam. 5 (1966) 363-367.
- [68] Bakker, R. J.; Dubessy, J.; Cathelineau, M.; “Improvements in clathrate modelling: I. The H₂O-CO₂ system with various salts”; Cosmochim. Geochim. Acta 60 (1960) 1657-1681.
- [69] Bakker, R. J.; “Improvements in clathrate modelling II: the H₂O-CO₂-CH₄-N₂-C₂H₆ fluid system”; in: Henriot, J.-P.; Mienert, J. (eds.); “Gas Hydrates: Relevance to World Margin Stability and Climate Change”; Geological Society, London, Special Publications 137 (1998) 75-105.